Electronic Supplementary Information

Controlling Orthogonal Self-Assembly through Cis-Trans Isomerization of a Non-Covalent Palladium Complex Dimer

Zoran Kokan,* Borislav Kovačević, Zoran Štefanić, Pavleta Tzvetkova, and Srećko I. Kirin*

E-mail: Zoran.Kokan@irb.hr, Srecko.Kirin@irb.hr

Table of Contents

Experimental Procedures

General Methods

Reactions were carried out in ordinary glassware and chemicals were used as purchased from commercial suppliers without further purification. Organic reactions were monitored by TLC on Silica Gel 60 F254 plates and detected with UV lamp (254 nm); organic compounds were purified using automated flash chromatography equipped with a UV detector (254 nm) and prepacked silica columns. NMR spectra were obtained on spectrometers operating at 300.13 or 600.13 MHz for ^{1}H, 242.93 MHz for ^{31}P, and 150.92 MHz for ^{13}C nuclei. The CD spectra were recorded on a JASCO J-810 spectropolarimeter equipped with Peltier thermostat. UV-Vis spectra were recorded on Varian Cary 50 spectrophotometer. FT-IR spectra were recorded on a Bruker Alpha-T FT-IR spectrometer using a Specac cell for liquid samples with 0.050 mm path length and CaF_2 windows. X-ray data was collected on a XtaLAB Synergy, Dualflex, HyPix diffractometer using Cu radiation and at the temperature of 100 K. The crystals diffracted rather weakly so the long exposures of 115 seconds were used. The data collection was further complicated by crystal twinning. The data collection and refinement parameters are given in Table S 4. Using Olex2,[1] the structure was solved with the ShelXS[2] structure solution program using Direct Methods and refined with the ShelXL[3] refinement package using Least Squares minimisation. Bulk solvent correction was used in the refinement because of the significant portion of the unit cell is occupied by disordered solvent (2690 Å^3, Figure S 46).[4] The data have been deposited at the Cambridge Crystallographic Data Centre under the following deposition number, CCDC 1564071. For details on DFT calculations see the "DFT Calculations" section.

Synthetic Procedures

Ligand synthesis and characterisation (**1a–c**) was done according to the literature procedure, and published elsewhere.[5]

Synthesis of **2a**

Bis-(acetonitrile)dichloropalladium (8.25 mg, 31.8 µmol) and **1a** (43.38 mg, 67.5 µmol) were dissolved in 4 mL of dichloromethane with 0.5 mL of methanol and left at room temperature overnight. The solvent was evaporated and a solid orange-yellow product was obtained in quantitative yield (by NMR). ^{1}H NMR (600.14 MHz, chloroform-d_1) δ/ppm: 3.07 (dd, 2H, J_1 = 8.5 Hz, J_2 = 14 Hz), 3.28 (dd, 2H, J_1 = 8 Hz, J_2 = 14 Hz), 3.34–3.38 (m, 4H), 4.51–4.55 (m, 2H), 5.46–5.50 (m, 2H), 5.96 (s, 2H), 6.09 (s, 2H), 6.99–7.04 (m, 8H), 7.07–7.15 (m, 8H), 7.30–7.37 (m, 12H), 7.48 (t, 2H, J = 7.5 Hz), 7.54 (t, 2H, J = 7.5 Hz), 7.59 (t, 2H, J = 4.5 Hz), 7.68–7.75 (m, 10H), 8.05 (s, 2H), 8.36 (s, 2H), 8.47 (d, 2H, J = 9 Hz), 8.52 (d, 2H, J = 3 Hz), 9.36 (d, 2H, J = 9 Hz). ^{13}C NMR (150.93 MHz, chloroform-d_1) δ/ppm: 36.5 (βPhe1), 37.4 (βPhe1), 52.7 (αPhe2), 55.3 (αPhe1), 126.1 (4Phe2), 126.4 (4Phe1), 126.84 (t, J = 26 Hz, 1Ph2), 127.6 (t, J = 24 Hz, 1Ph1), 128.1 (4), 128.2 (3Phe2), 128.3 (3Phe1), 128.6 (t, J = 5.5 Hz, 3Ph2), 128.87 (t, J = 5.5 Hz, 3Ph1), 128.93 (2Phe2), 129.2 (2Phe1), 131.1 (4Ph1), 131.3 (t, J ≈ 25 Hz, overlapping, 1), 131.4 (4Ph2), 133.2 (2), 133.4 (t, J = 5 Hz, 3'), 133.7 (d, J = 3 Hz, 3), 134.1 (t, J = 5.5 Hz, 2Ph1), 136.9 (t, J = 6.5 Hz, 2Ph2), 137.5 (1Phe2), 137.7 (1Phe1), 138.9 (t, J = 8 Hz, 2'), 165.6 (5'), 169.2 (5), 172.0 (6'), 173.7 (6). ^{1}H NMR (600.14 MHz, acetonitrile-d_3) δ/ppm: 3.13 (dd, 4H, J_1 = 13.5 Hz, J_2 = 8 Hz, *cis*-), 3.25 (dd, 4H, J_1 = 13.5 Hz, J_2 = 7.5 Hz, *cis*-), 4.63–4.67 (m, 4H, *cis*-), 6.70 (s, 8H, overlapping diffuse C-terminal amides, *cis*-), 7.22–7.26 (m, 8H, *cis*-), 7.29–7.34 (m, 12H), 7.39–7.43 (m, 12H), 7.50–7.54 (m, 4H), 7.55–7.59 (m, 4H), 7.92–7.96 (m, 4H), 8.01–8.02 (m, 2H). ^{1}H NMR (600.14 MHz, methanol-d_4) δ/ppm: 3.13 (dd, 4H, J_1 = 9 Hz, J_2 = 13.5 Hz, *cis*-), 3.27 (dd, 4H, J_1 = 7 Hz, J_2 = 13.5 Hz, *cis*-), 4.71 (dd, 4H, J_1 = 7 Hz, J_2 = 8.5 Hz, *cis*-), 7.09–8.19 (non-trivial assignation due to overlapping signals). ^{31}P NMR (242.93 MHz, chloroform-d_1) δ/ppm: 25.00 (s). ^{31}P NMR (242.93 MHz, acetonitrile-d_3) δ/ppm: 23.97 (s, *trans*-**2a**), 32.42 (s, *cis*-**2a**). ^{31}P NMR (242.93 MHz, methanol-d_4) δ/ppm: 24.34 (s, *trans*-**2a**), 33.46 (s, *cis*-**2a**), 33.75 (s, a possible conformer of *cis*-**2a**). ^{31}P NMR (242.93 MHz, 1,1,2,2-tetrachloroethane-d_2) δ/ppm: 24.09 (s, *trans*-**2a**), 32.70 (s, *cis*-**2a**).

Synthesis of **2b**

Bis-(acetonitrile)dichloropalladium (10.27 mg, 39.6 µmol) and **1b** (55.72 mg, 82.8 µmol) were dissolved in 6 mL of dichloromethane, sonicated for 3 min, and left at room temperature overnight. The solvent was evaporated and a solid orange product was obtained in quantitative yield (by NMR). ^{1}H NMR (600.14 MHz, chloroform-d_1) δ/ppm: 3.03 (dd, 4H, J_1 = 7 Hz, J_2 = 14 Hz, *trans*-), 3.17 (dd, 4H, J_1 = 6 Hz, J_2 = 14 Hz, *trans*-), 3.68 (s, 12H, *trans*-), 4.88–4.92 (m, 4H, *trans*-), 6.56 (d, 4H, J = 7.5 Hz, *trans*-), 7.04–8.02 (assignation non-trivial due to overlapping signals from *cis*- and *trans*-**2b** isomers). ^{1}H NMR (600.14 MHz, acetonitrile-d_3) δ/ppm: 3.02 (dd, 4H, J_1 = 14 Hz, J_2 = 8.5 Hz, *trans*-), 3.20 (dd, 4H, J_1 = 14 Hz, J_2 = 5.5 Hz, *trans*-), 3.65 (s, 12H, *trans*-), 4.76–4.80 (m, 4H, *trans*-), 7.14–8.07 (assignation non-trivial due to overlapping signals from *cis*- and *trans*-**2b** isomers). ^{31}P NMR (242.93 MHz, chloroform-d_1) δ/ppm: 23.64 (s, *trans*-**2b**), 32.44 (s, *cis*-**2b**). ^{31}P NMR (242.93 MHz, acetonitrile-d_3) δ/ppm: 23.97 (s, *trans*-**2a**), 32.42 (s, *cis*-**2a**). ^{31}P NMR (242.93 MHz, methanol-d_4) δ/ppm: 24.96 (s, *trans*-**2b**), 34.16 (s, *cis*-**2b**).

Synthesis of **2c**

Bis-(acetonitrile)dichloropalladium (4.39 mg, 16.9 μmol) and **1c** (16.66 mg, 34.0 μmol) were dissolved in 6 mL of dichloromethane with 0.5 mL of methanol, sonicated for 1 min, and left at room temperature overnight. The solvent was evaporated and a solid orange product was obtained in quantitative yield (by NMR). ^{1}H NMR (600.14 MHz, acetonitrile-d_3) δ/ppm: 1.45 (d, 12H, *J* = 7.5 Hz, *cis*-), 4.39–4.44 (m, 4H, *cis*-), 6.24 (ws, 4H, *cis*-), 6.68 (s, 4H, *cis*-), 7.42–7.56 (m, 16H), 7.60–7.63 (m, 6H), 7.99–8.02 (m, 4H, *cis*-), 8.09–8.10 (m, 2H, *cis*-). ^{1}H NMR (600.14 MHz, methanol-d_4) δ/ppm: 1.52 (d, 12H, *J* = 7.5 Hz), 4.45 (q, 4H, *J* = 7.5 Hz), 7.43–7.67 (m, 20H), 8.00–8.03 (m, 4H), 8.26–8.27 (m, 2H). ^{31}P NMR (242.93 MHz, acetonitrile-d_3) δ/ppm: 26.56 (s, *trans*-**2c**), 33.04 (s, *cis*-**2c**). ^{31}P NMR (242.93 MHz, methanol-d_4) δ/ppm: 25.31 (s, *trans*-**2c**), 31.44 (s, **1c**-oxide), 33.94 (s, *cis*-**2c**), 34.56 (s, a possible conformer of *cis*-**2c**).

Results and Discussion

NMR Measurements

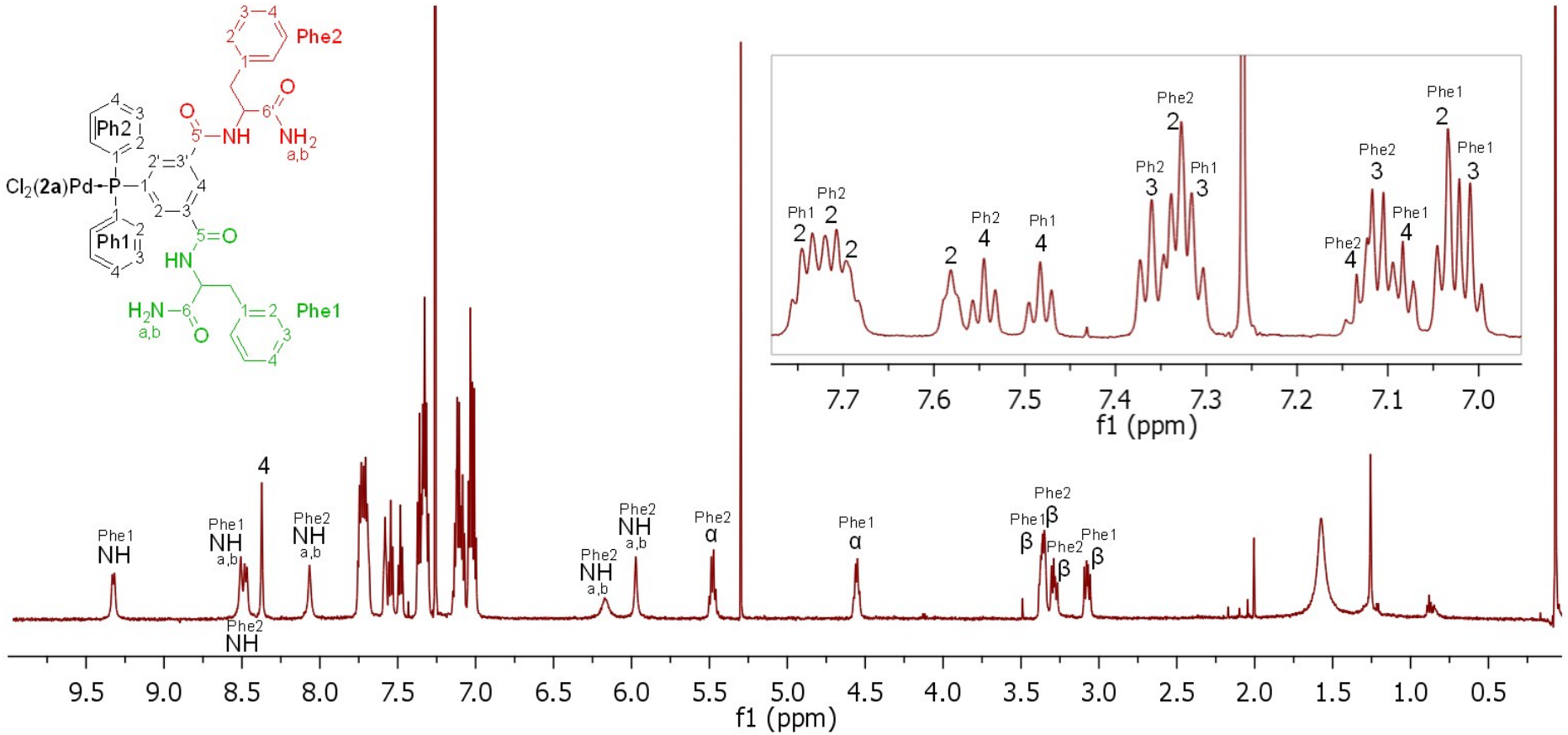

Figure S 1. ^{1}H NMR (chloroform-d_1) spectra of *trans*-**2a**.

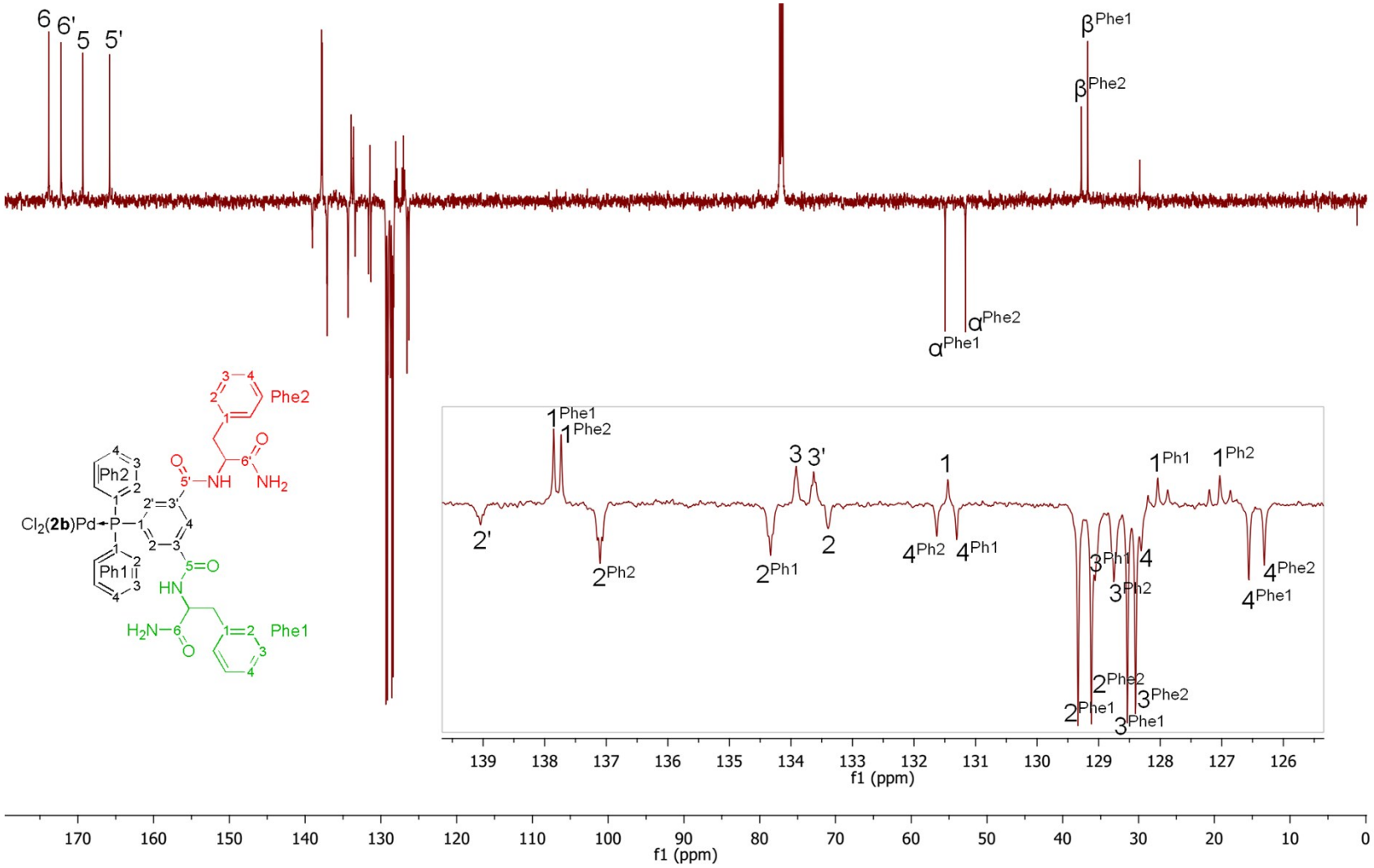

Figure S 2. ^{13}C NMR (chloroform-d_1) APT spectra of *trans*-**2a**.

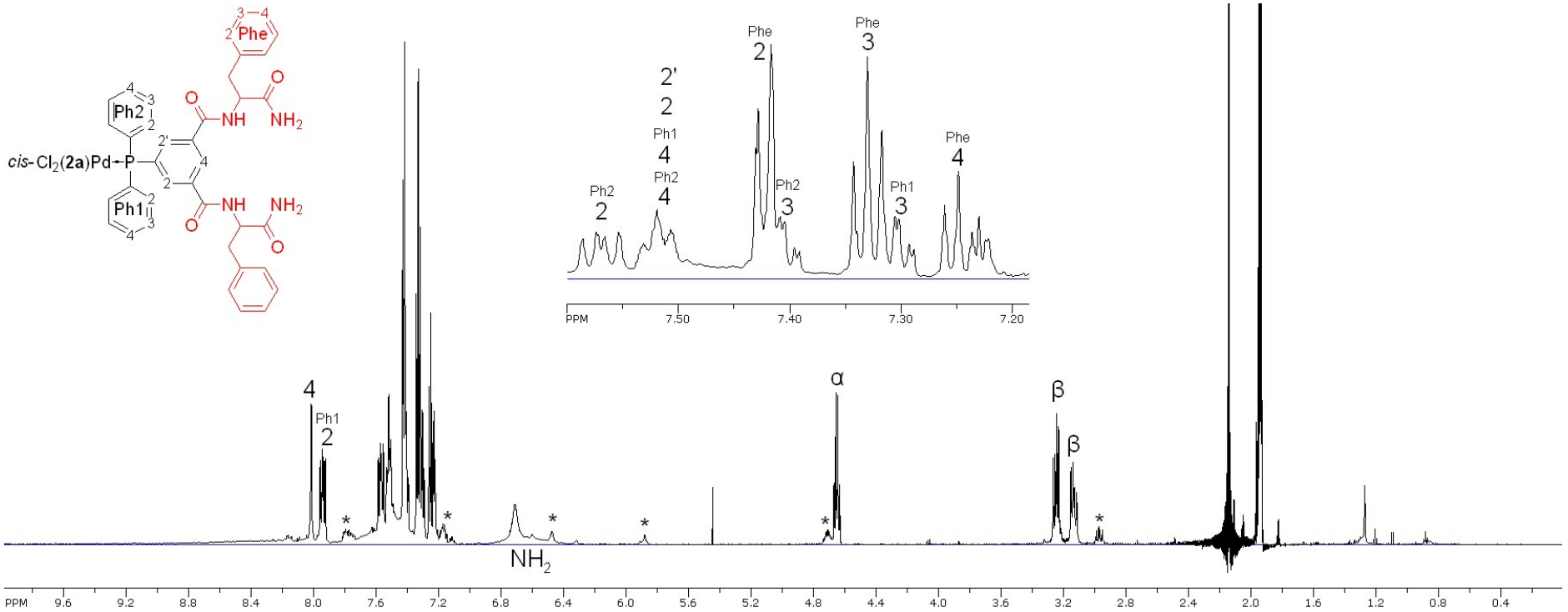

Figure S 3. ^{1}H NMR (acetonitrile-d_3) spectra of *cis*-**2a**. Small amount (≈ 20 %) of *cis*-conformer is visible (asterisk).

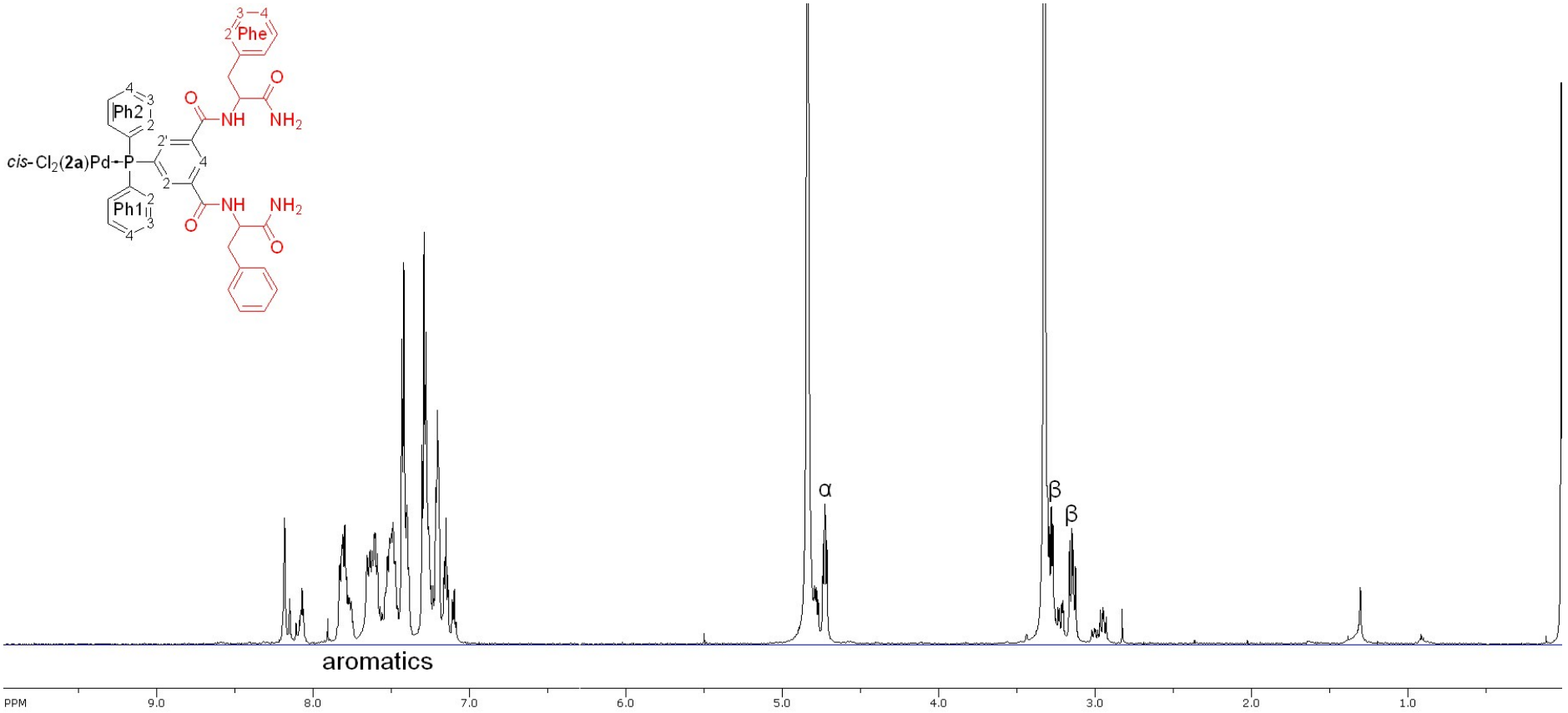

Figure S 4. ^{1}H NMR (methanol-d_4) spectra of *cis*-**2a**. Around 30 % of *trans*-isomer is visible. Nontrivial assignation of aromatics due to severe signal overlap.

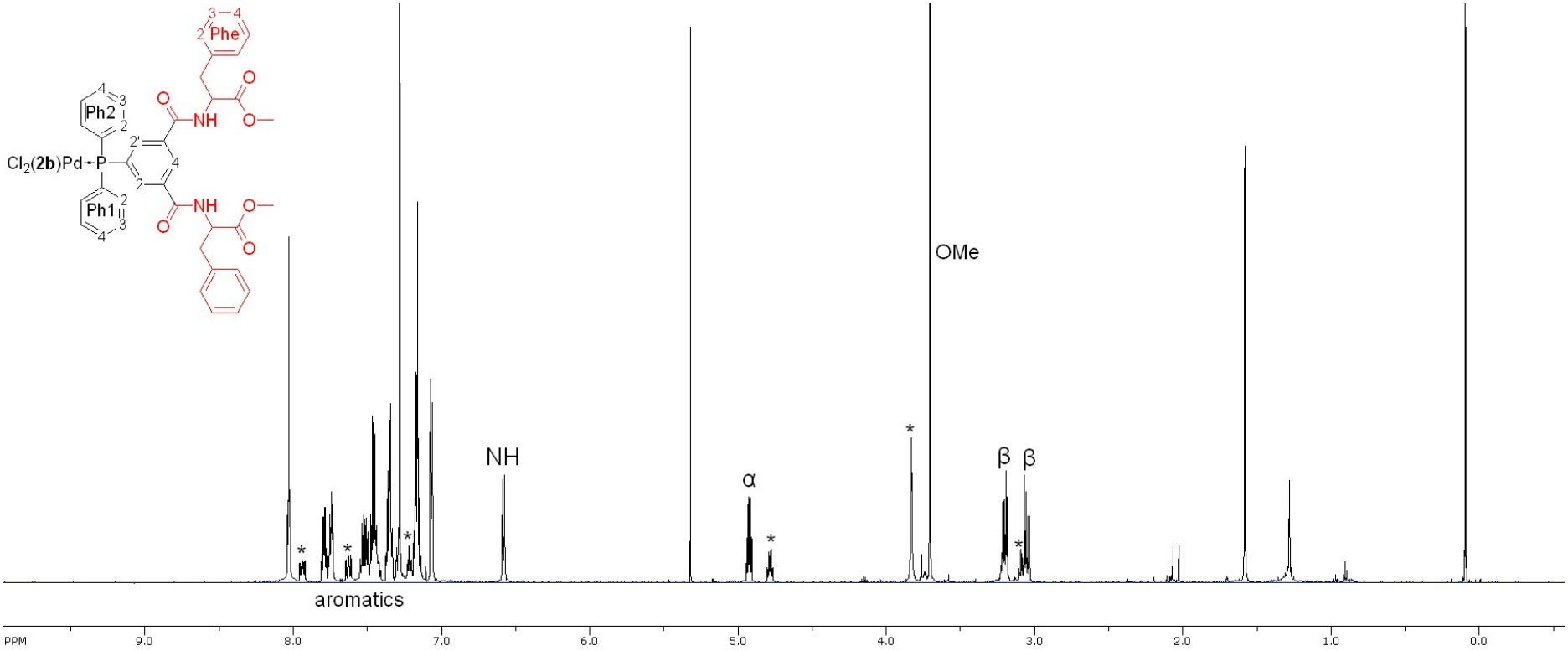

Figure S 5. ^{1}H NMR (chloroform-d_1) spectra of **2b**. Some signals of the *cis*-isomer are marked with asterisk. Nontrivial assignation of aromatics due to severe signal overlap.

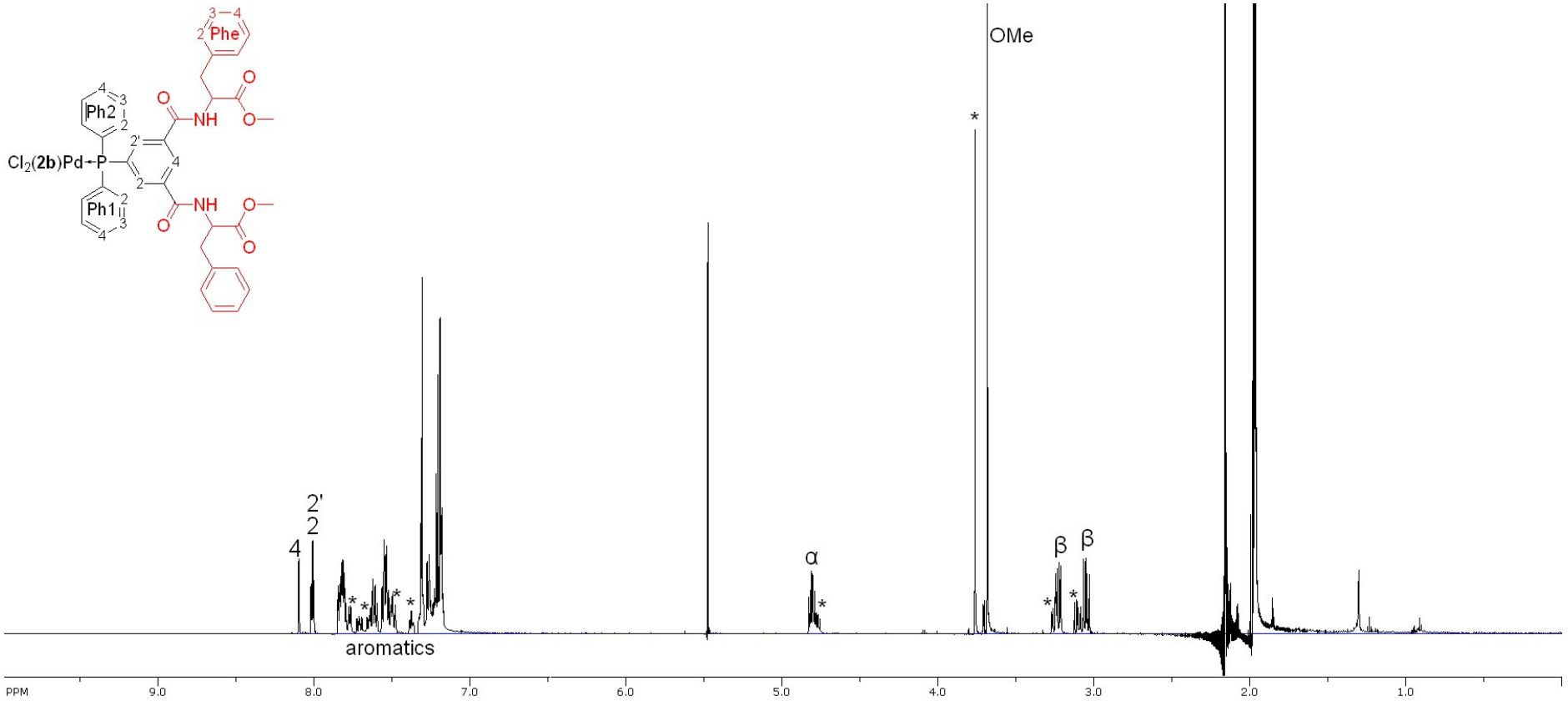

Figure S 6. ^{1}H NMR (acetonitrile-d_3) spectra of **2b**. Some signals of the *cis*-isomer are marked with asterisk. Nontrivial assignation of aromatics due to severe signal overlap.

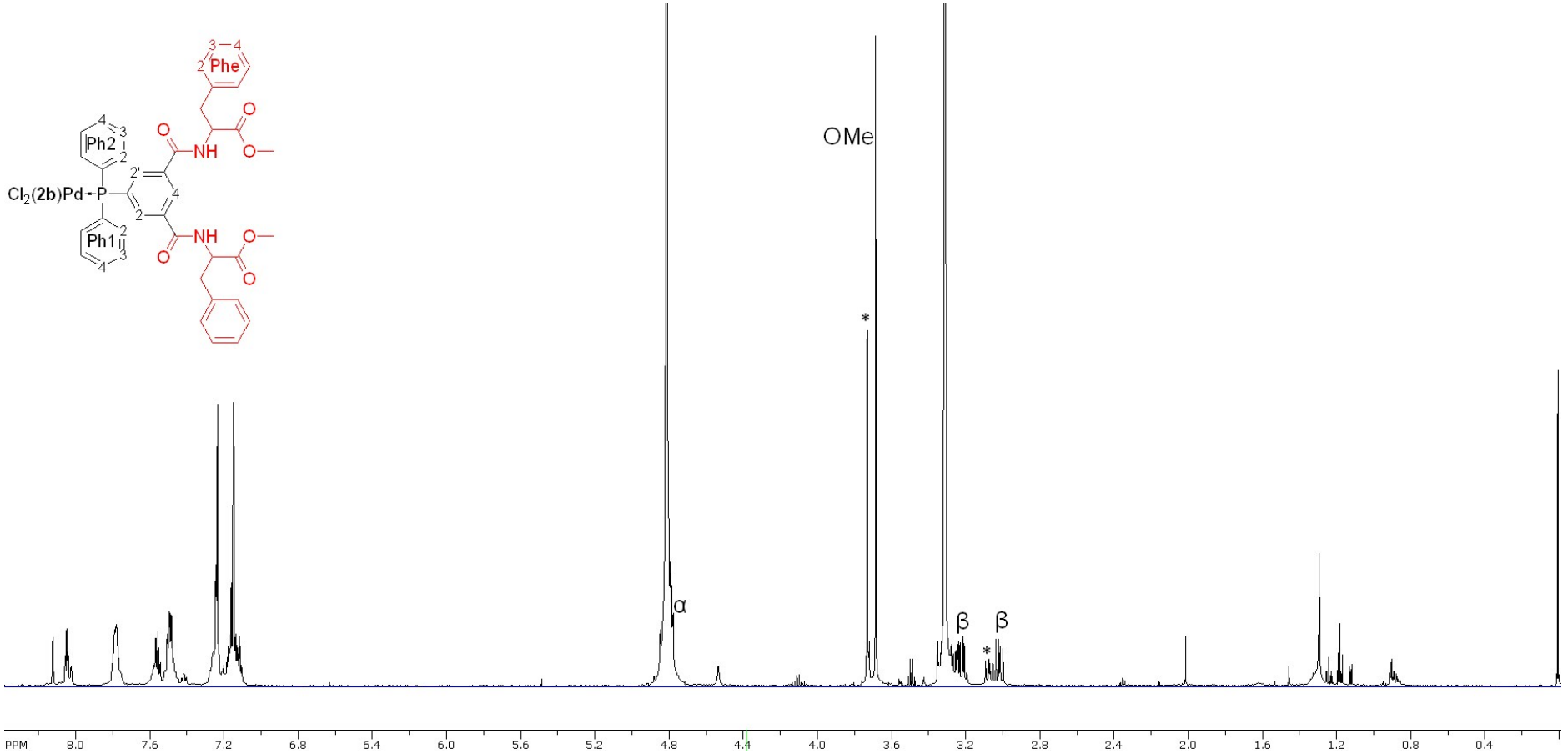

Figure S 7. ^{1}H NMR (methanol-d_4) spectra of **2b**. Some signals of the *cis*-isomer are marked with asterisk. Nontrivial assignation of aromatics due to severe signal overlap.

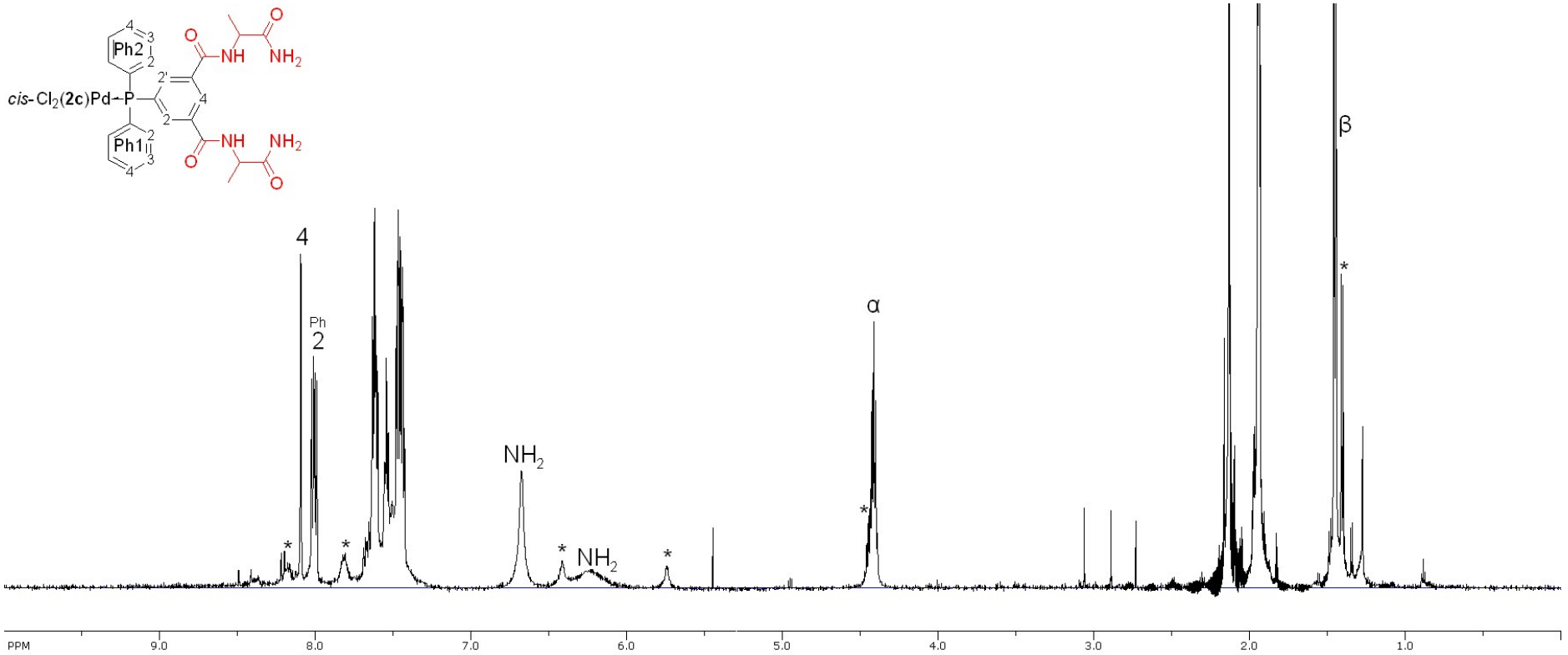

Figure S 8. Assigned ^{1}H NMR (acetonitrile-d_3) spectra of *cis*-**2c**. A small amount of *cis*-conformer is visible and marked with asterisk. Nontrivial assignation of aromatics due to severe signal overlap.

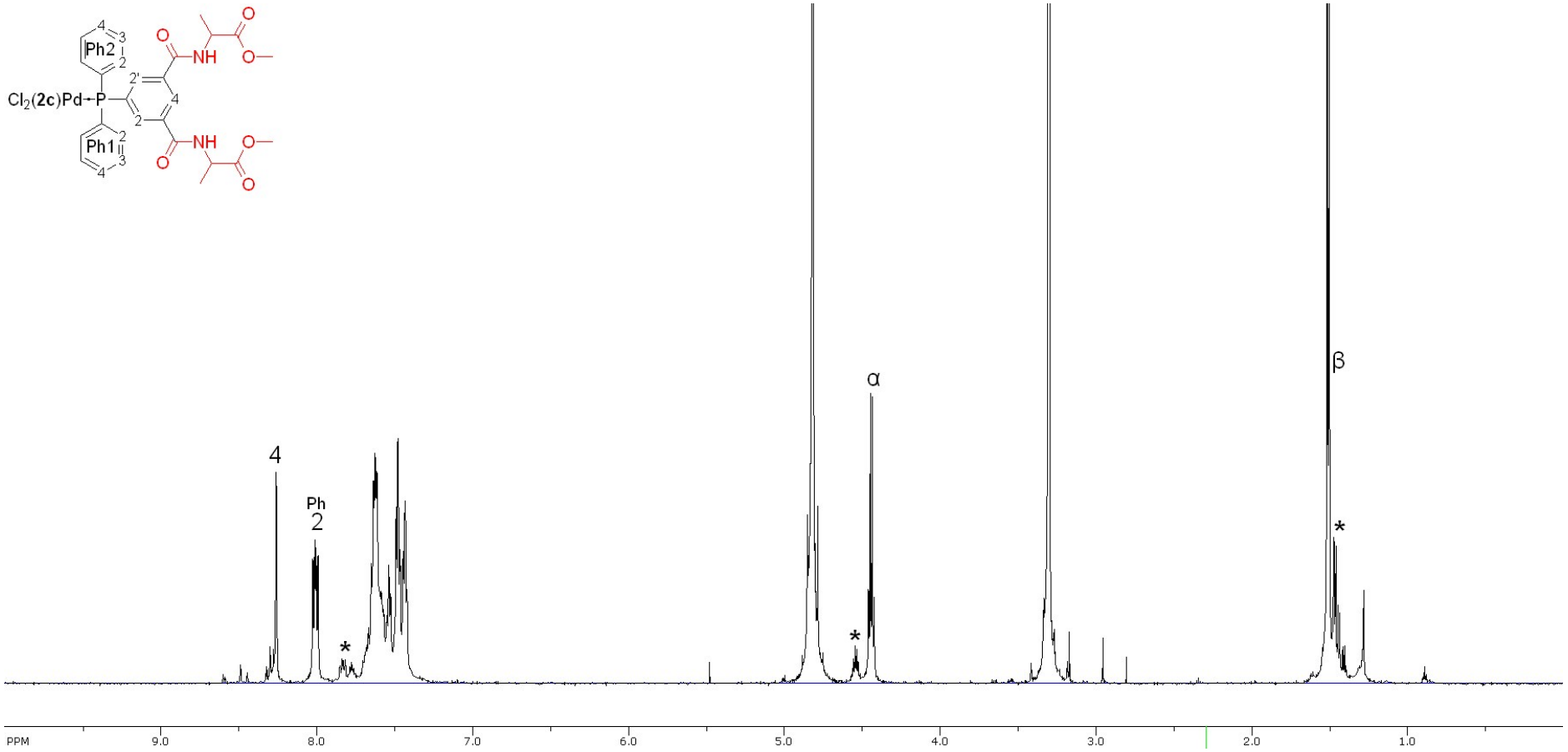

Figure S 9. Assigned ^{1}H NMR (methanol-d_4) spectra of *cis*-**2c**. A small amount of *cis*-conformer/*trans*-isomer is visible and marked with asterisk. Nontrivial assignation of aromatics due to severe signal overlap.

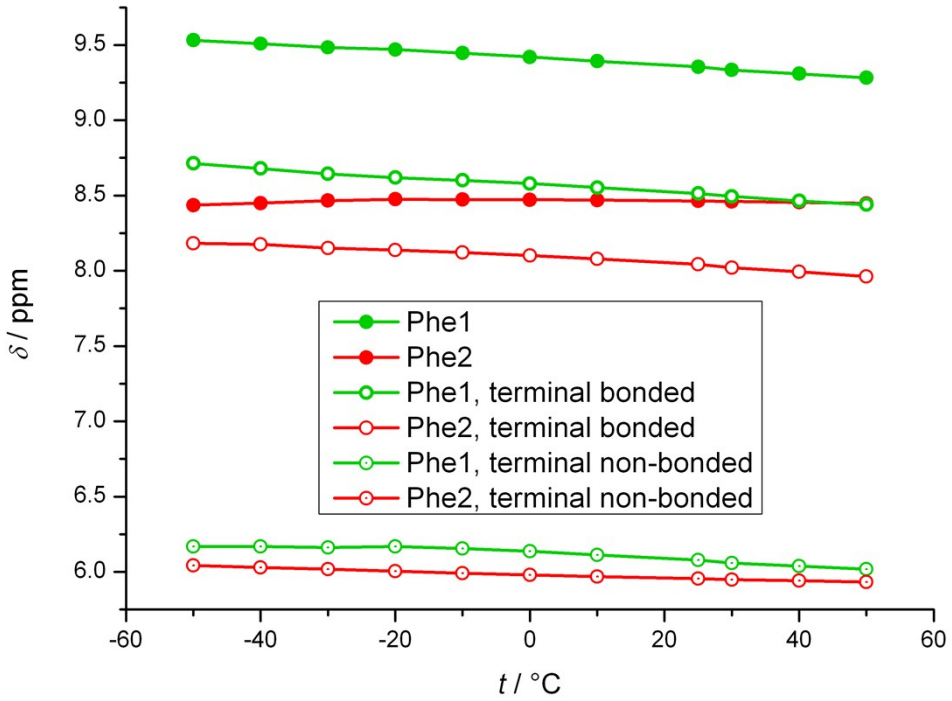

Figure S 10. Temperature dependence of the amide proton chemical shifts of **2a** in chloroform-d_1 (*C*-terminal amides are abbreviated with "terminal"; Different phenyalanines are colour indicated). All the amide protons do not shift significantly throughout wide temperature range. Low temperature coefficients of the hydrogen-bonded amides ($\delta > 7$ ppm) are similar and fairly linear (≈ 2.8 ppb K^{-1} in a 0–60 °C temperature range), except for Phe2 amide (0.5 ppb K^{-1}), nevertheless indicative of hydrogen-bonded amides shielded from the solvent molecules.[6]

Table S 1. Cis-isomer abundance in various solvents for complexes **2**.

Compound	*cis*-isomer / %[(a)]		
	chloroform-d1	acetonitrile-d3	methanol-d4
2a	0	99[(b)]	78
2b	31	31	37
2c	insoluble	94[(b)]	93[(b)]

[(a)] the values were obtained by ^{1}H NMR integration. The values "0" or "100" mean that the cis- or trans-isomer, respectively, were not detected.

[(b)] the values were obtained by ^{31}P NMR integration

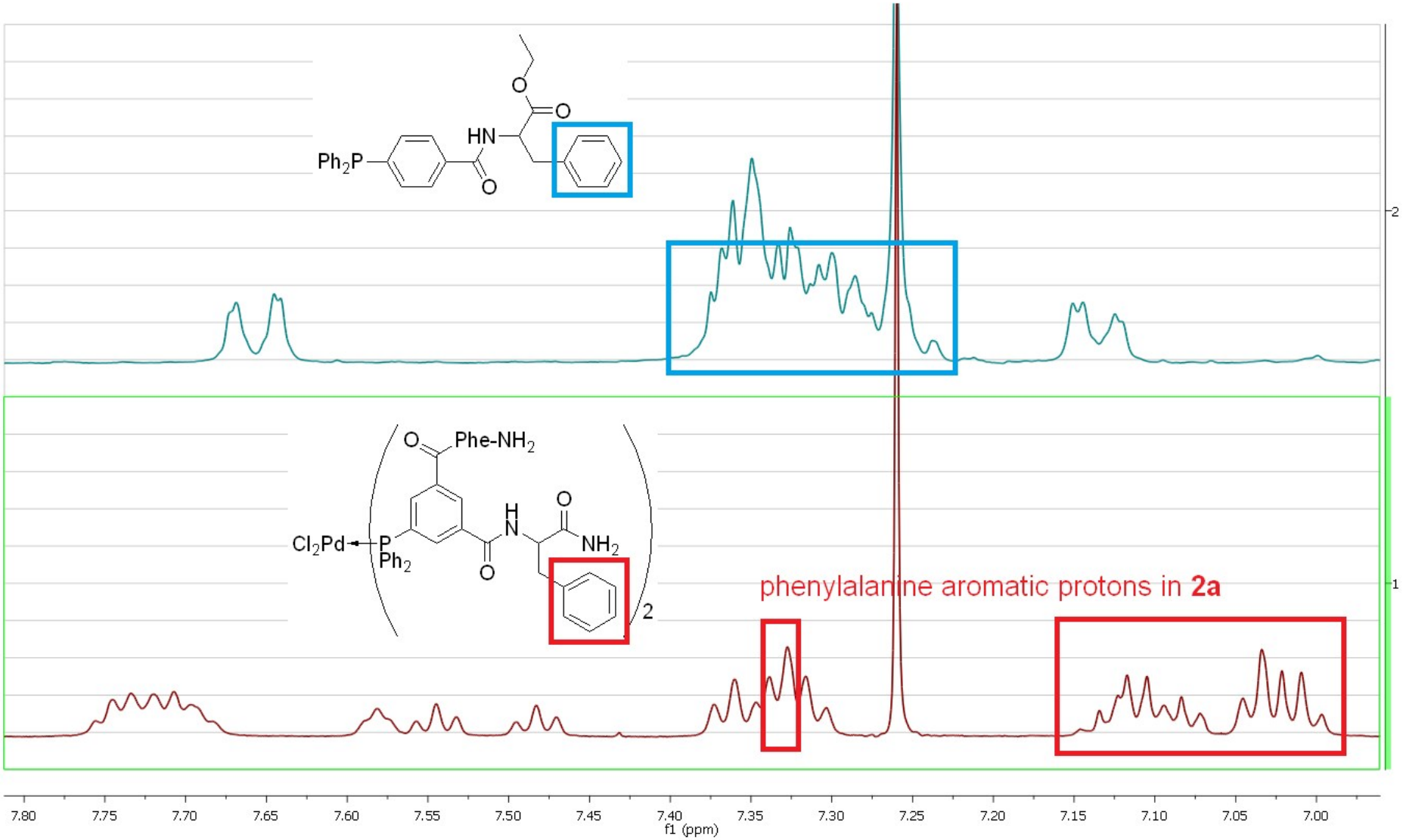

Figure S 11. ^{1}H NMR intercept (chloroform-d_1). Comparison of phenylalanine aromatic proton chemical shift in **2a** complex (bottom) and similar compound[7] (top) that does not form any supramolecular associates, indicates aromatic stacking in **2a**. For exact assignation see Figure S 1.

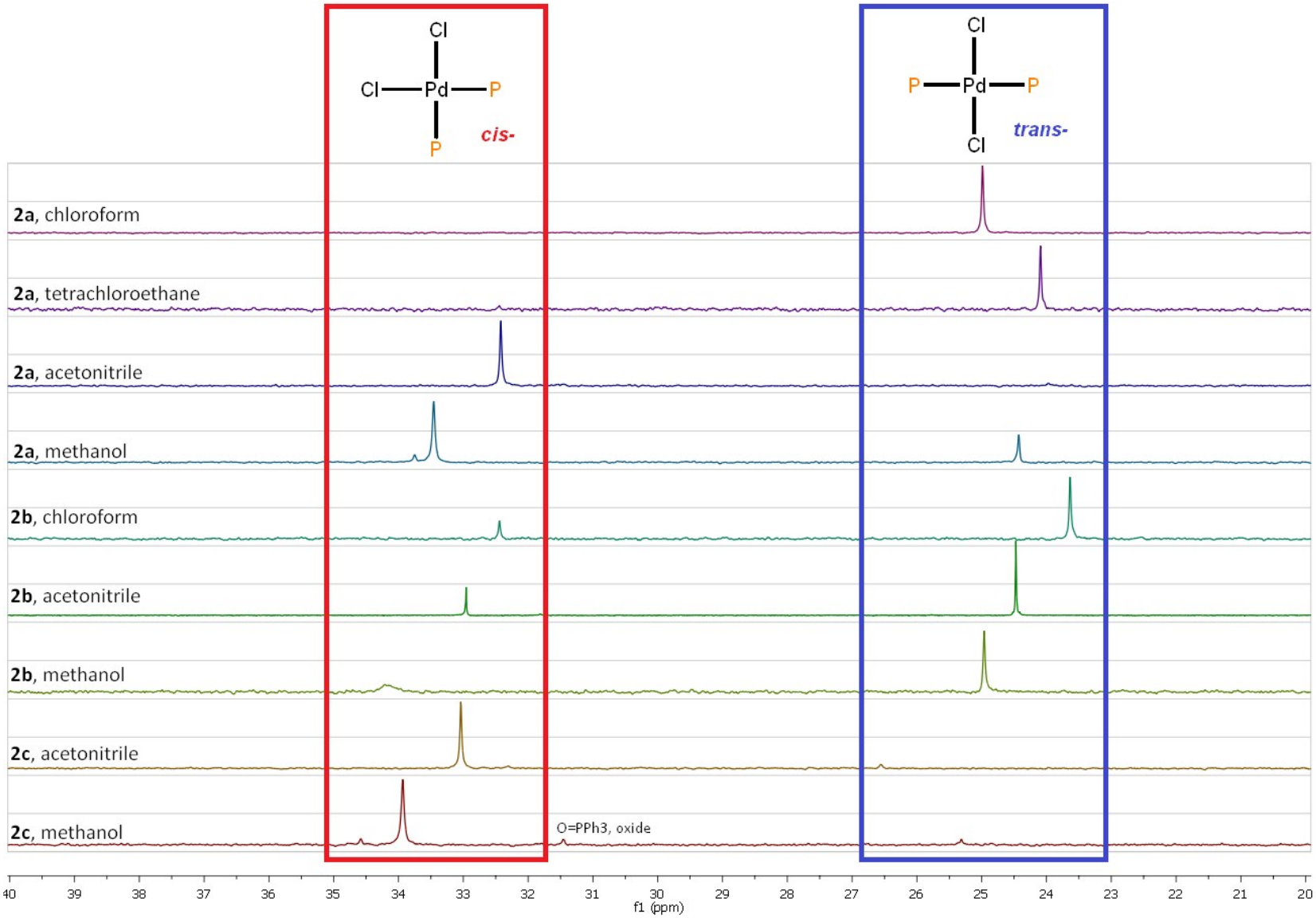

Figure S 12. ^{31}P NMR spectra of the palladium complexes, showing *cis*- and *trans*-isomers. Minor additional peaks in the cis-region in methanol may indicate a different conformer, since solvolysis of one chloride would substantially shift the phosphorous peaks downfield due to the formation of a cationic Pd species. No free ligand was observed (≈ –6 ppm).

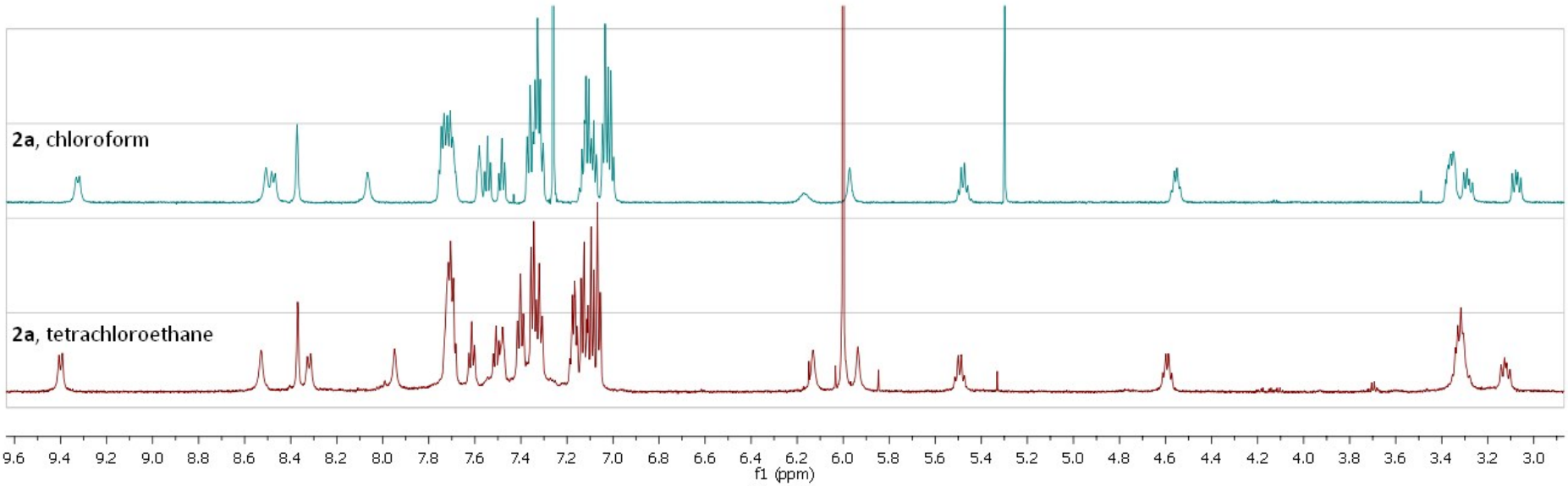

Figure S 13. ^{1}H NMR spectra comparison of **2a** in two chlorinated solvents, showing very similar characteristics, indicating that 1,1,2,2-tetrachloroethane also facilitates dimer formation. For detailed asignation see Figure S 1.

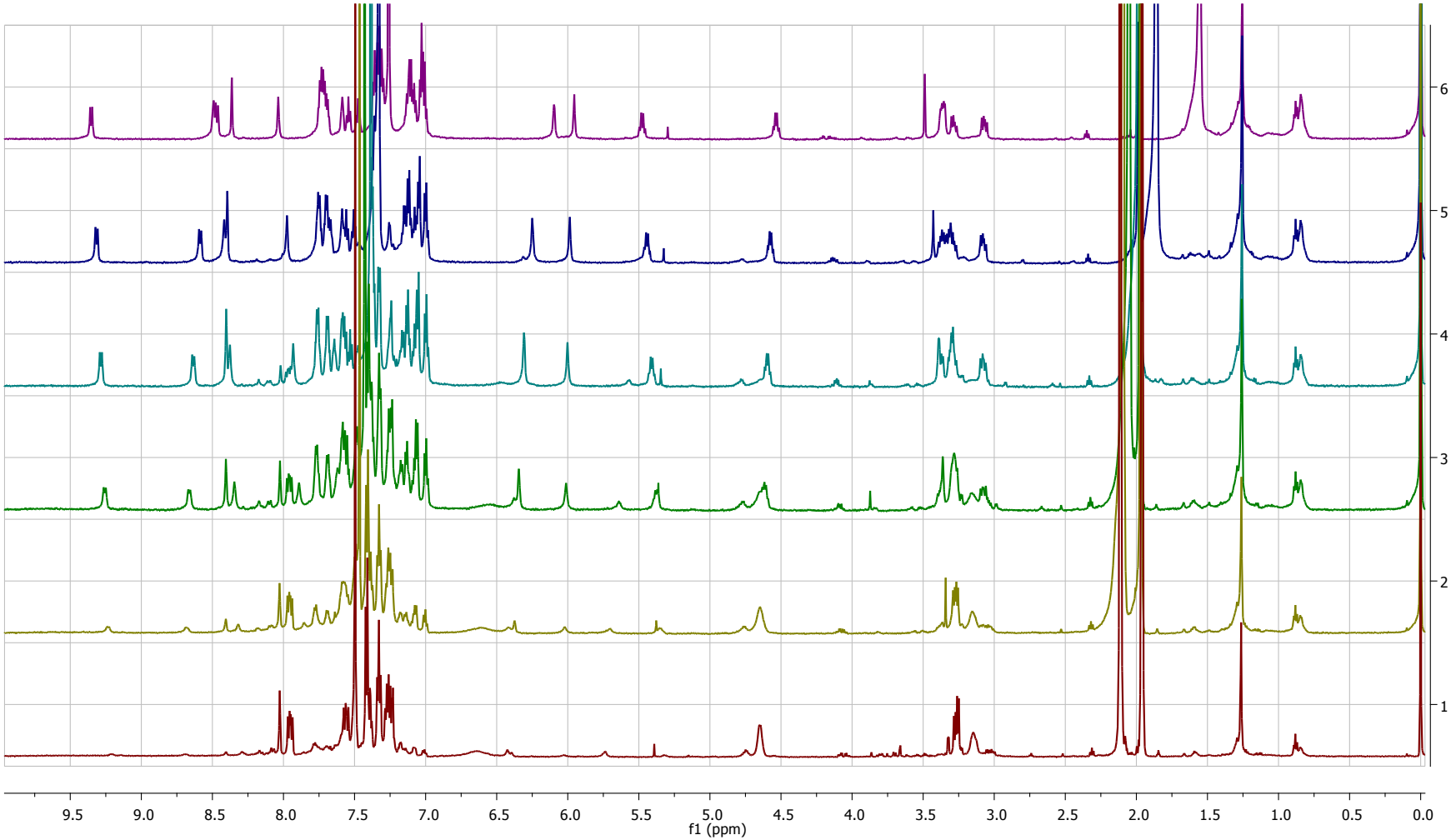

Figure S 14. Variable solvent composition ^{1}H NMR spectra of **2a** in chloroform with 0, 10, 20, 30, 40, and 50 % of acetonitrile (top to bottom). Small signal at 4.75 ppm (and its accompanying signals) in the bottom spectra does not belong to the dimeric species but is ascribed as a cis-conformer (≈ 20 % abundance by integration) since the phosphorous NMR shows only cis-**2a** peak (Figure S 15).

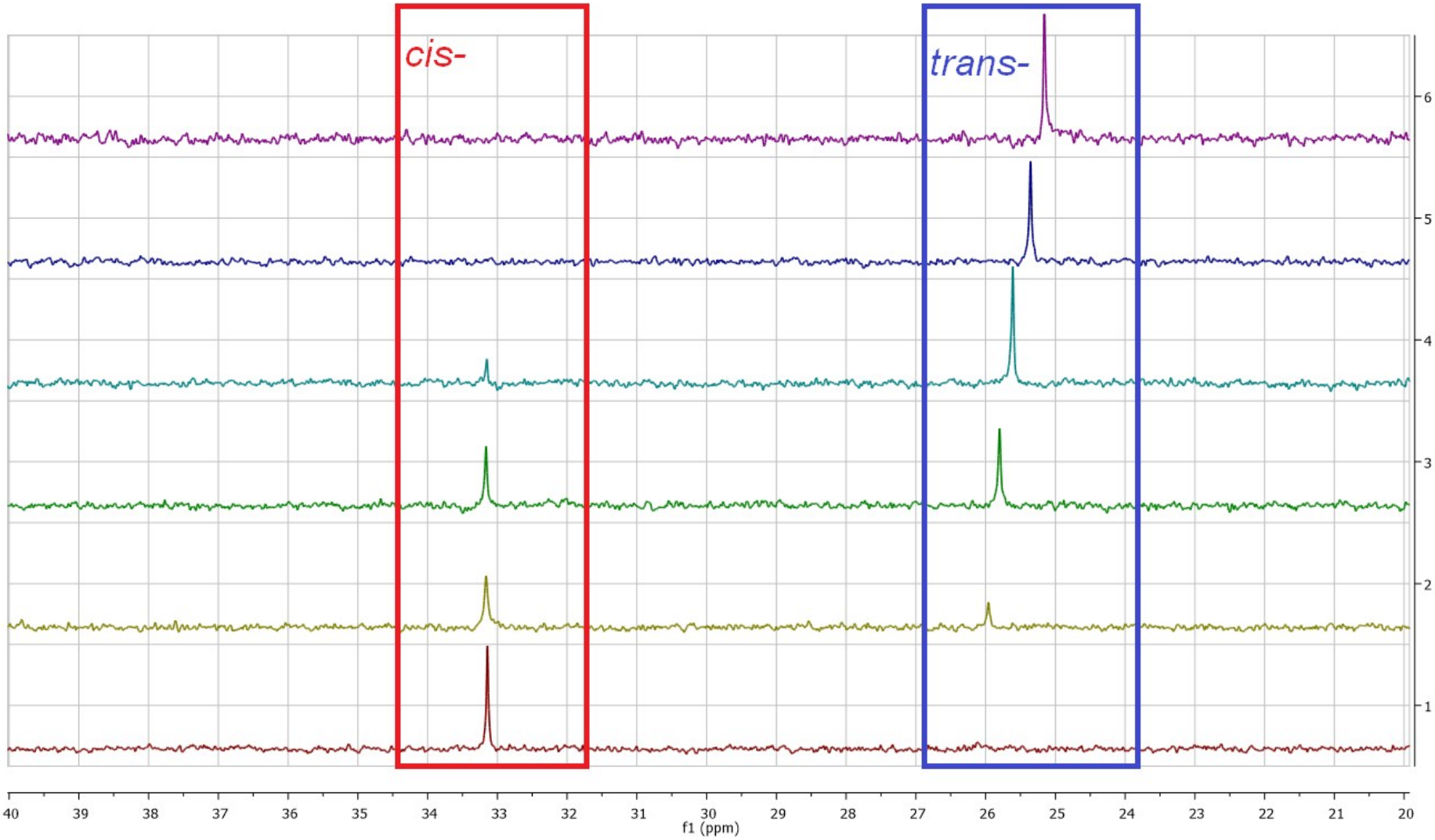

Figure S 15. Variable solvent composition ^{31}P NMR spectra of **2a** in chloroform with 0, 10, 20, 30, 40, and 50 % of acetonitrile (top to bottom) showing cis- and trans-isomers. No other peaks were detected in the range of –250 to +150 ppm.

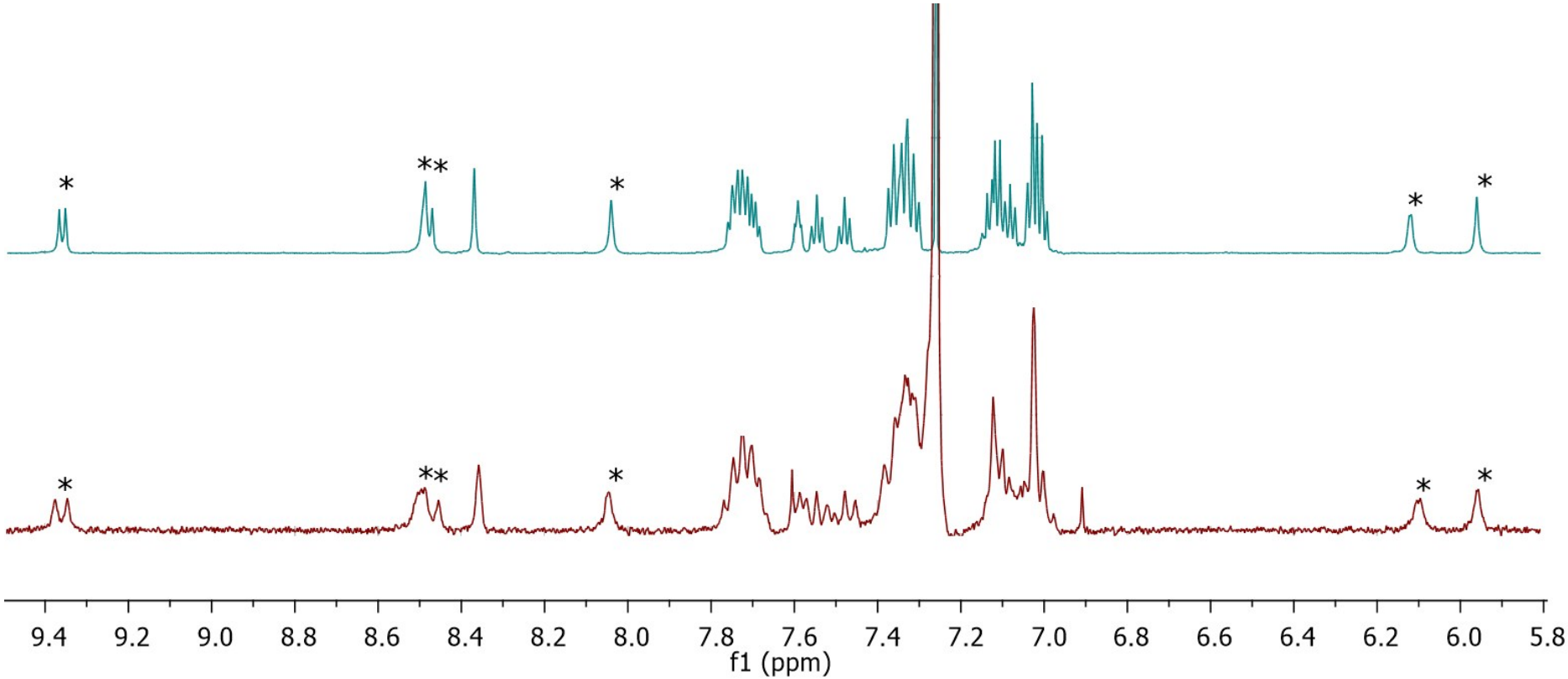

Figure S 16. ^{1}H NMR spectra (chloroform-d_1) of **2a** at 5.6 mM (top) and 0.5 mM (bottom) showing no significant shift of any amide protons (marked with asterisk). Top and bottom spectra were recorded at 600 and 300 mHz, respectively.

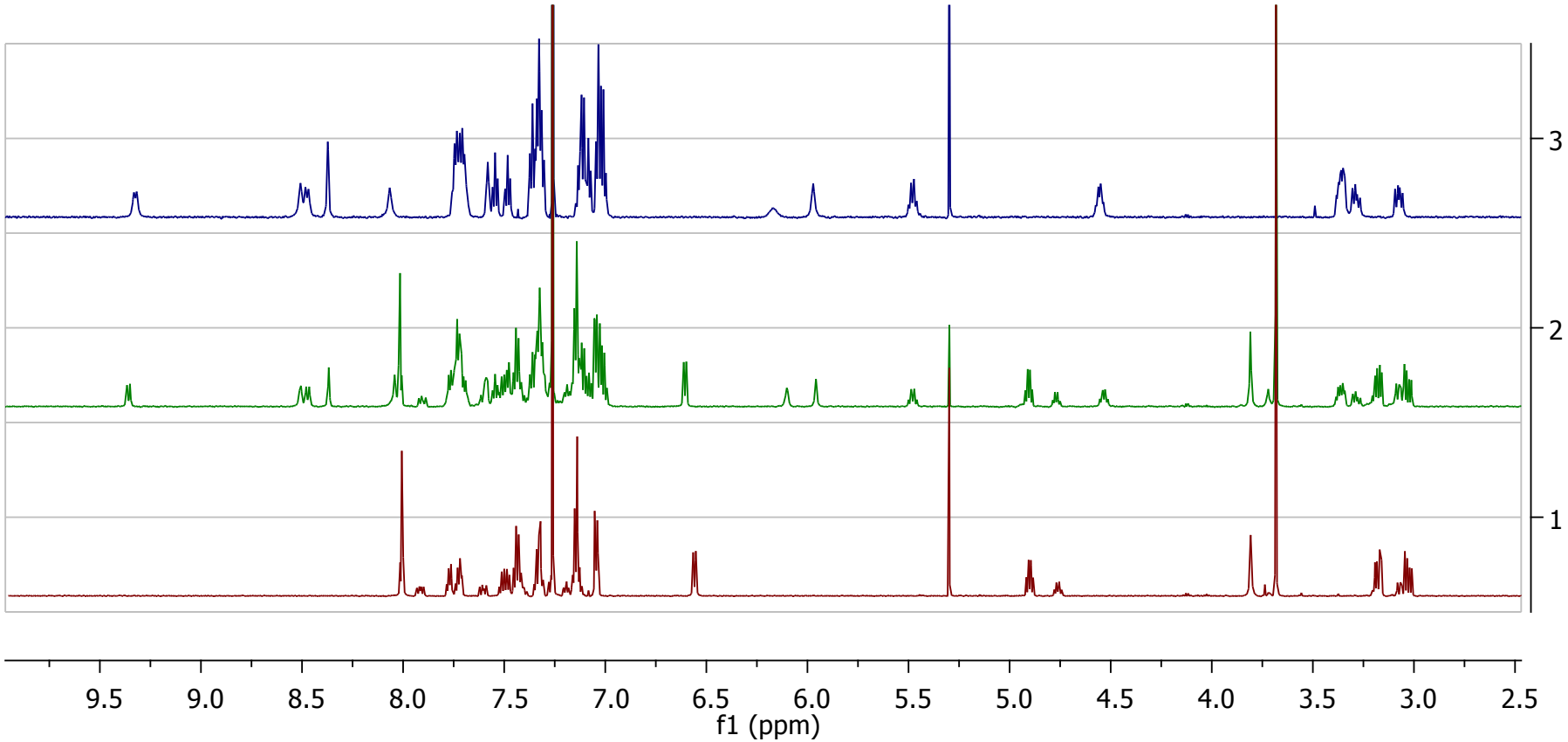

Figure S 17. ^{1}H NMR spectra of **2a** (top), **2b** (bottom), and 1:1 **2a**:**2b** mixture in chloroform, showing that the mixed experiment shows no significant proton shifting (as well the absence of additional peaks) with comparison to pure spectra, indicating that the two complexes are not involved in ligand exchange and act as independant species in solution.

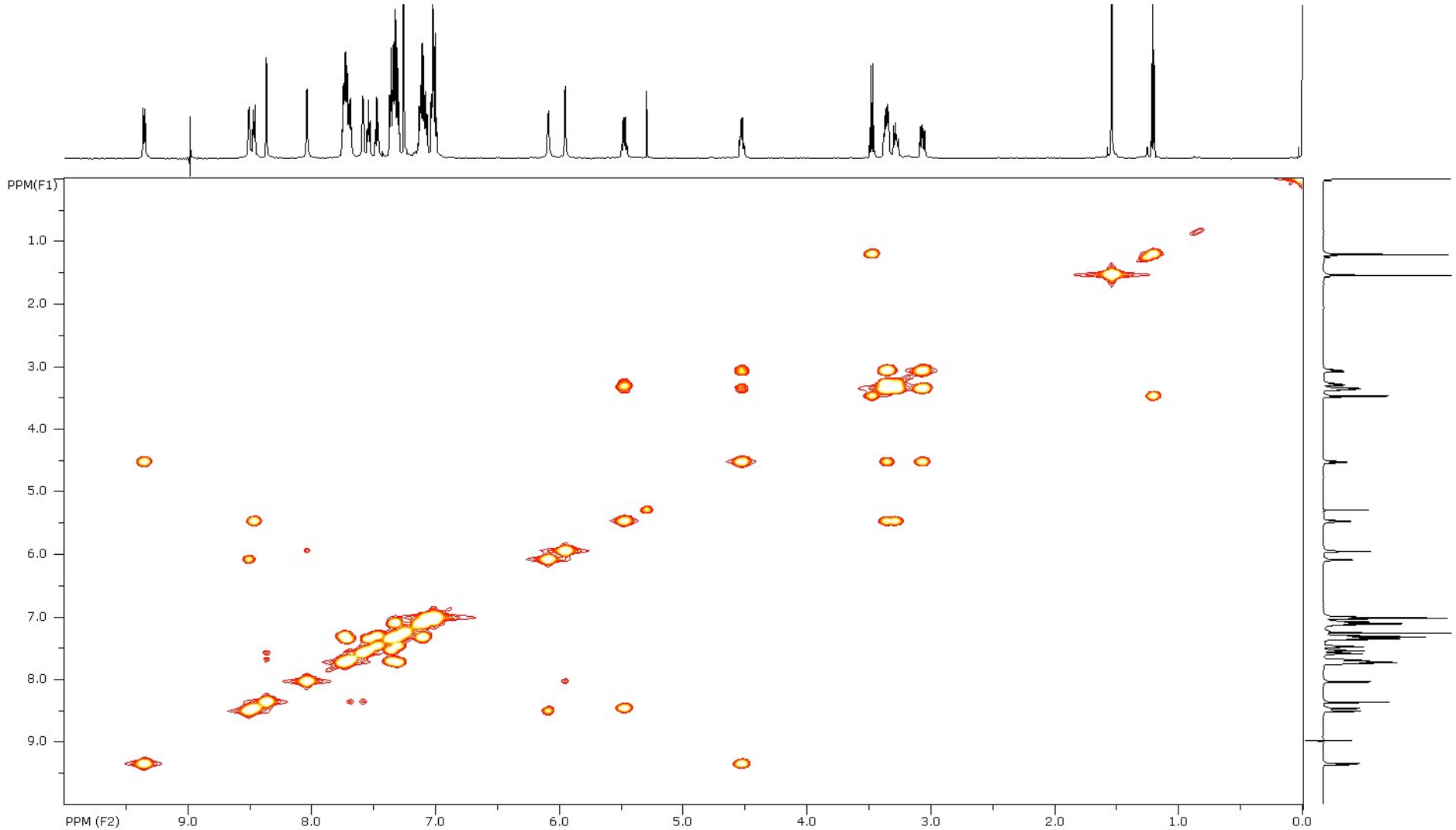

Figure S 18. ^{1}H COSY spectrum of **2a** in chloroform-d_1.

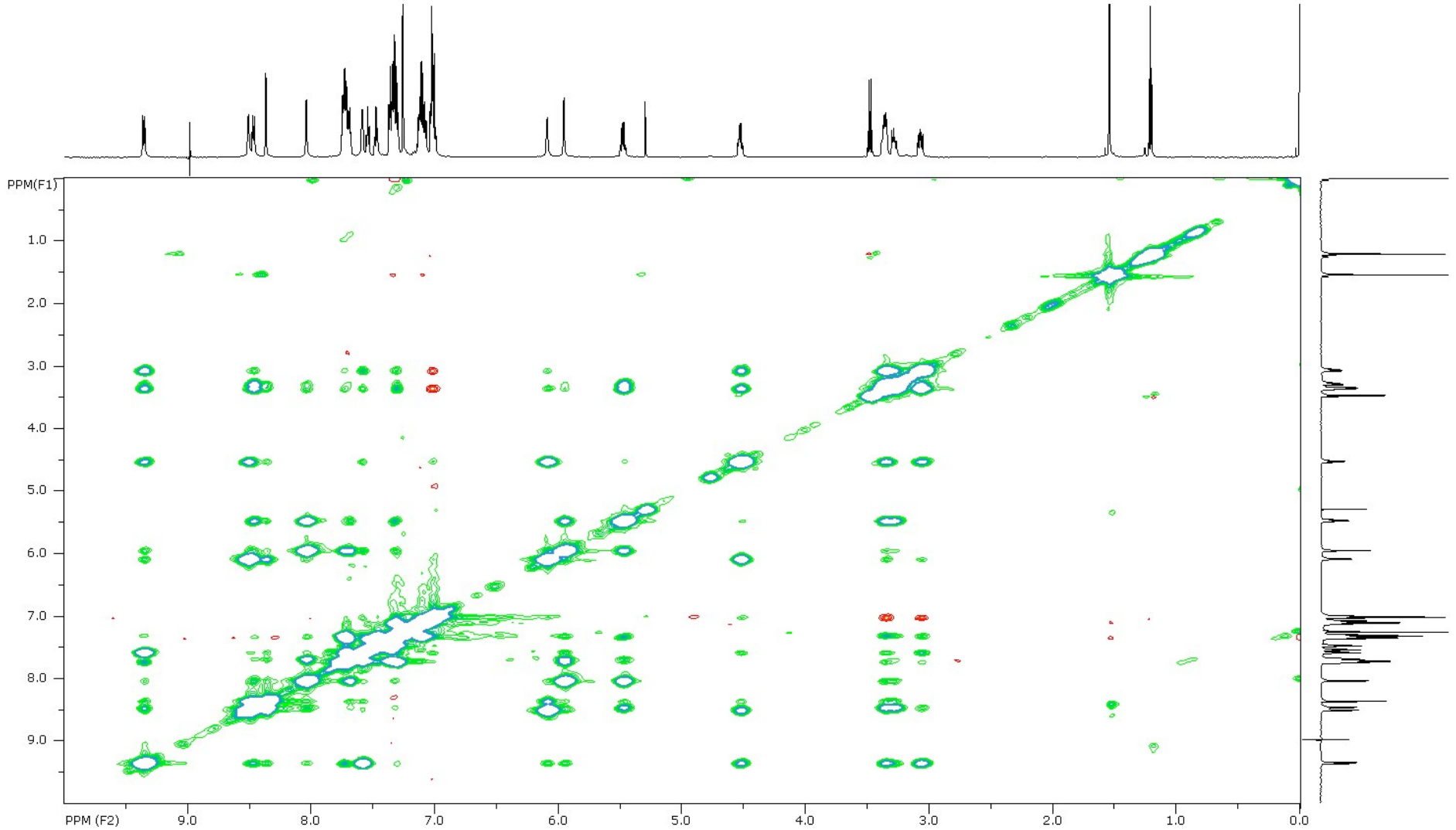

Figure S 19. ^{1}H NOESY spectrum of **2a** in chloroform-d_1. Mixing time, 600 ms.

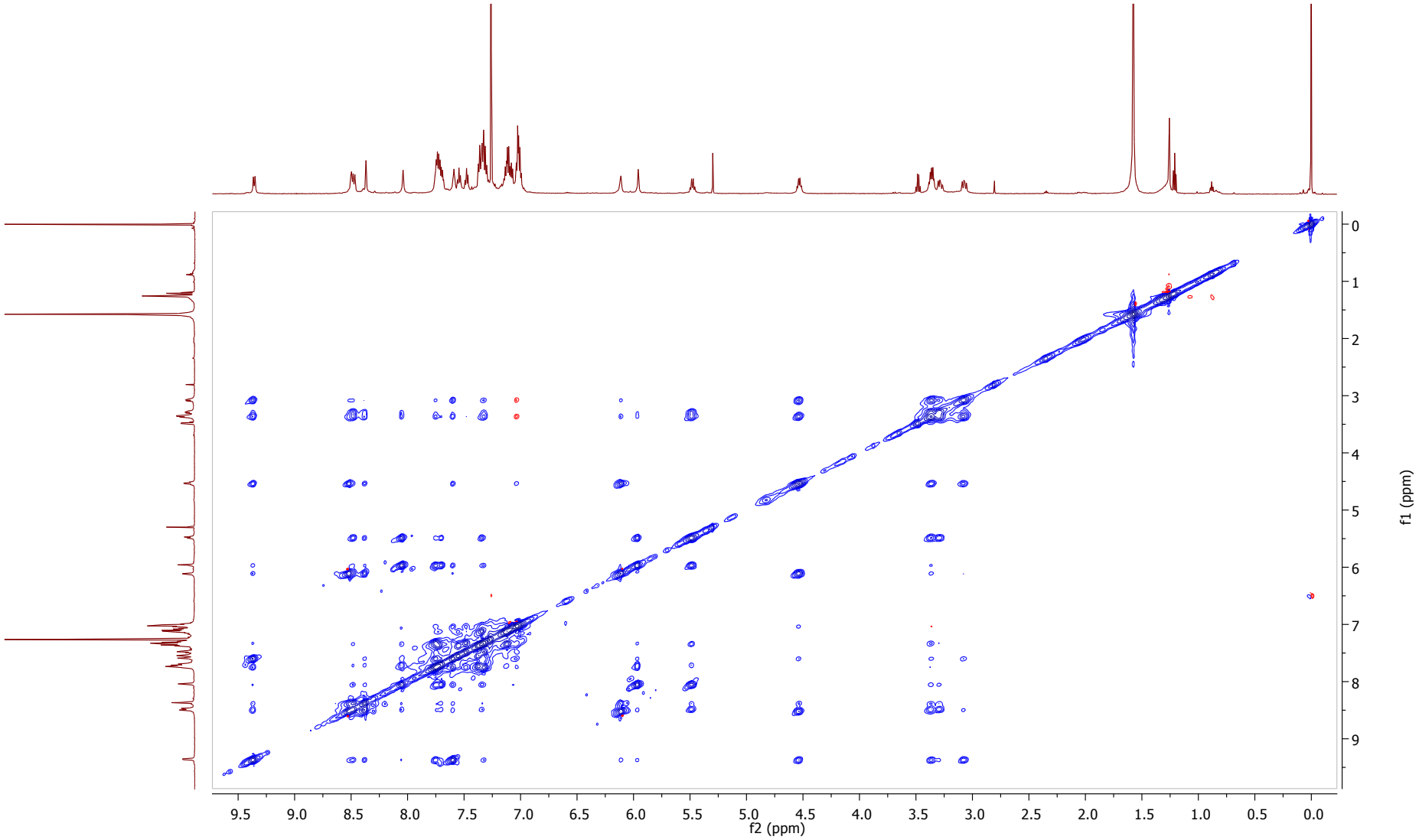

Figure S 20. ^{1}H NOESY spectrum of **2a** in chloroform-d_1. Mixing time, 900 ms.

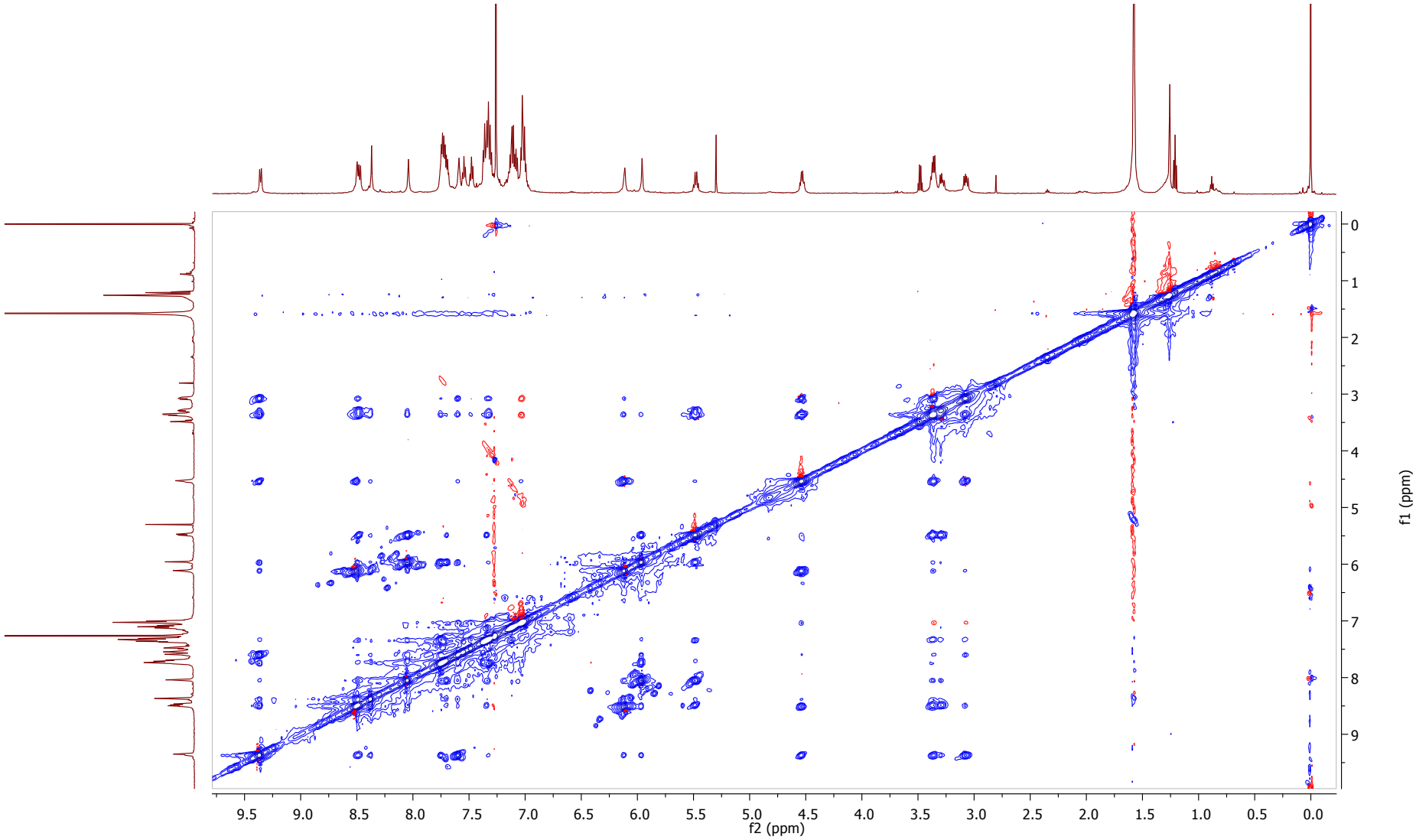

Figure S 21. ^{1}H NOESY spectrum of **2a** in chloroform-d_1. Mixing time, 200 ms.

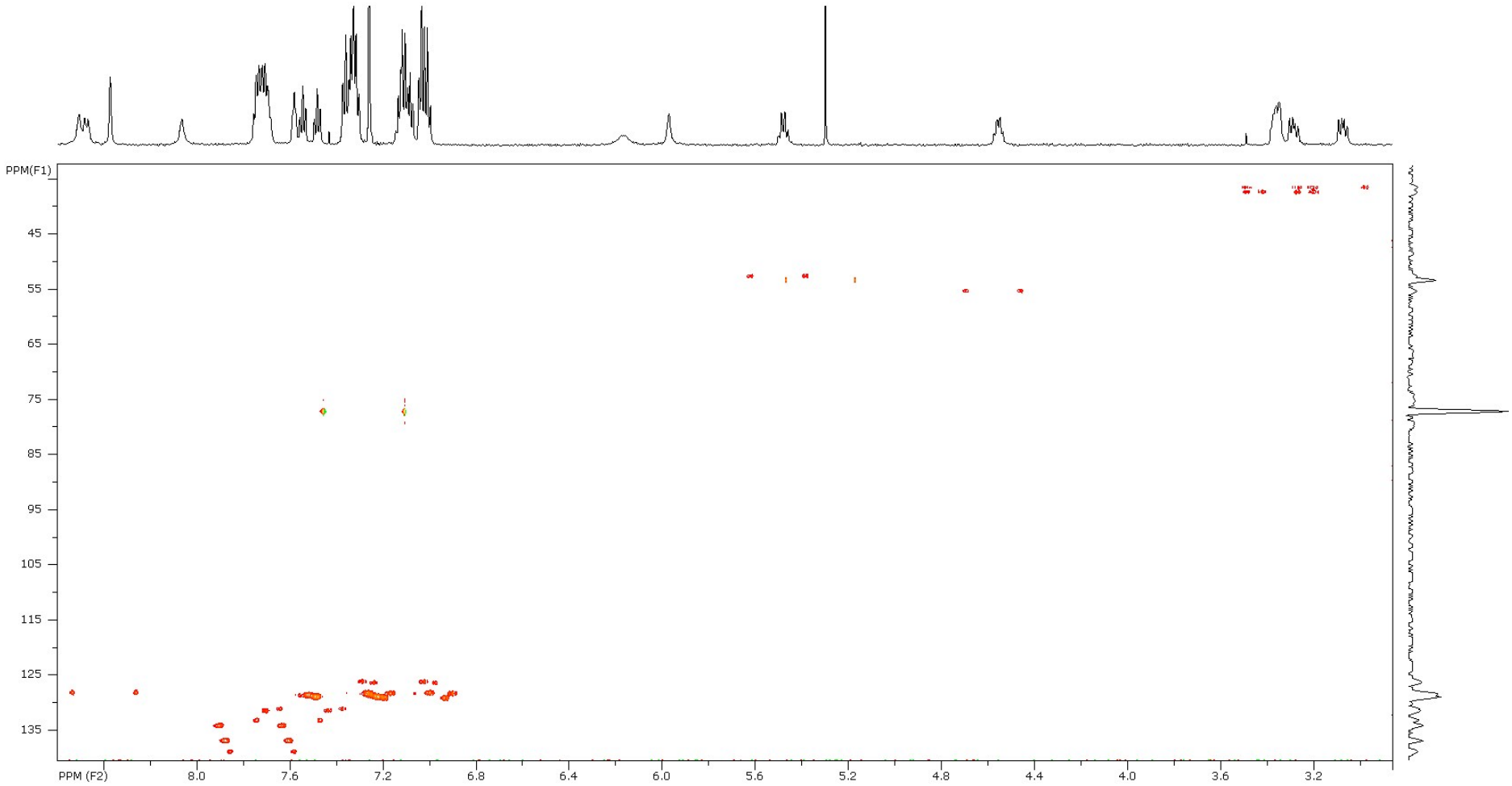

Figure S 22. F_2-coupled ^{1}H, ^{13}C HSQC spectrum of **2a** in chloroform-d_1.

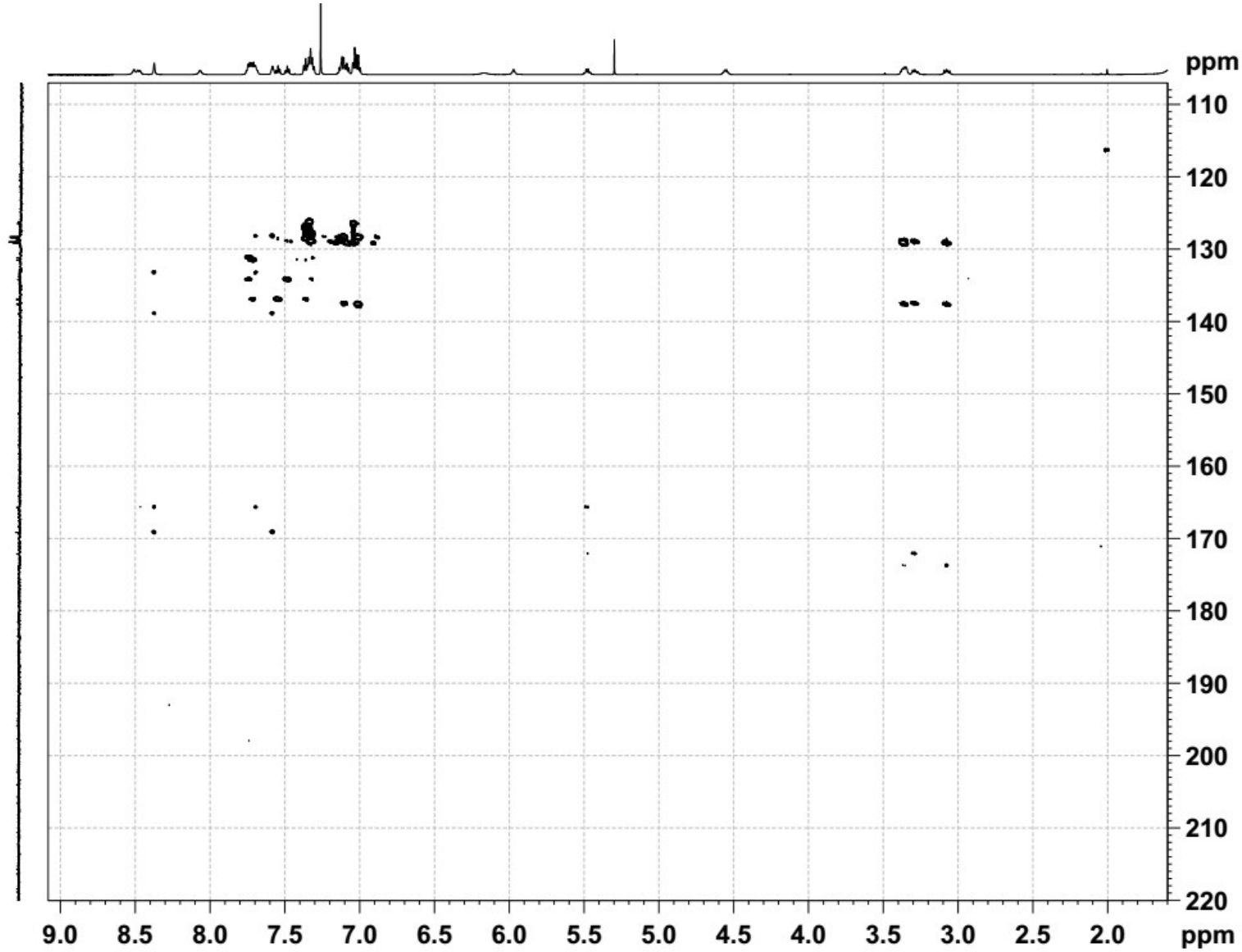

Figure S 23. ^{1}H, ^{13}C HMBC spectrum of **2a** (aromatic region) in chloroform-d_1.

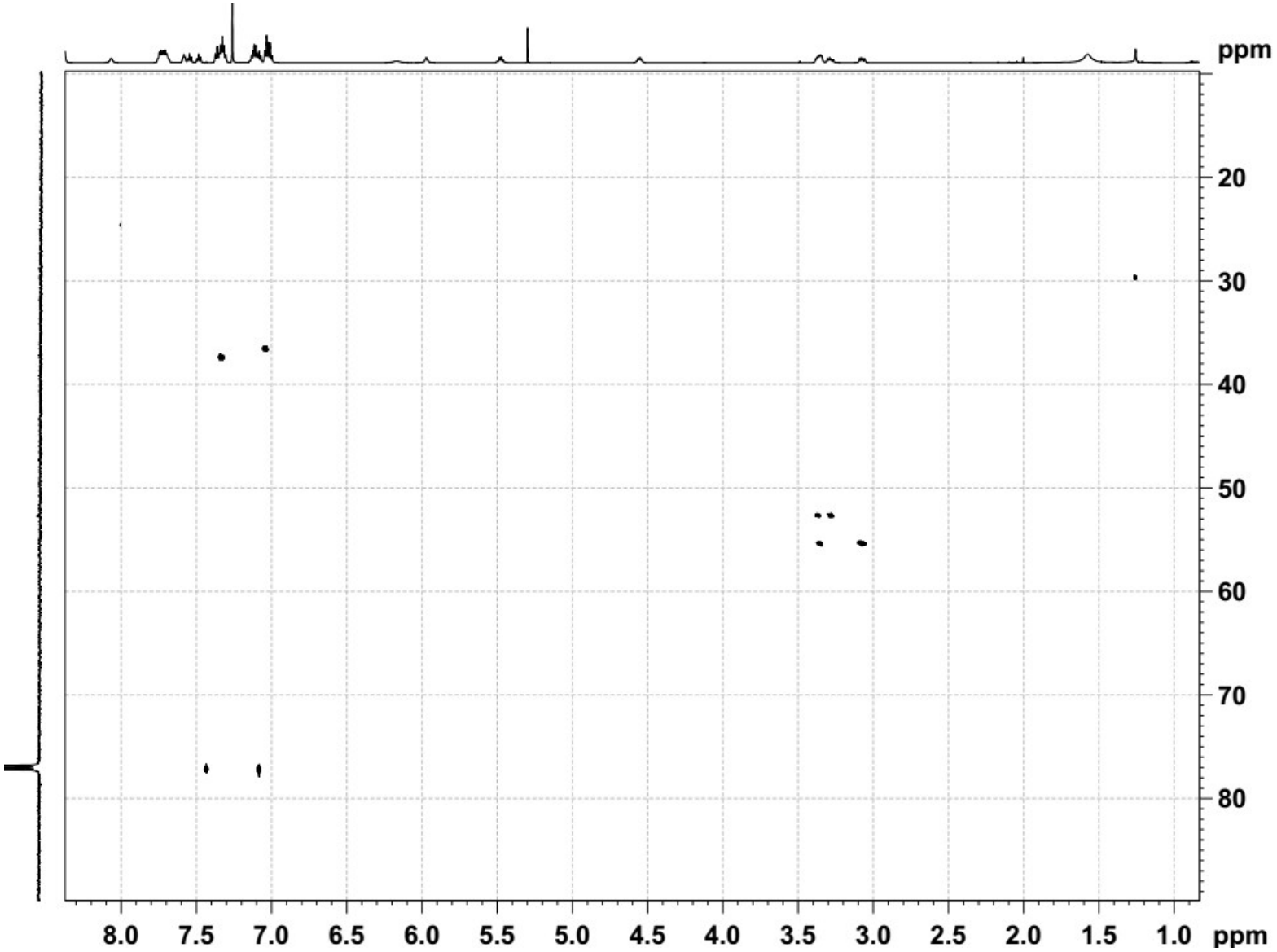

Figure S 24. ^{1}H, ^{13}C HMBC spectrum of **2a** (aliphatic region) in chloroform-d_1.

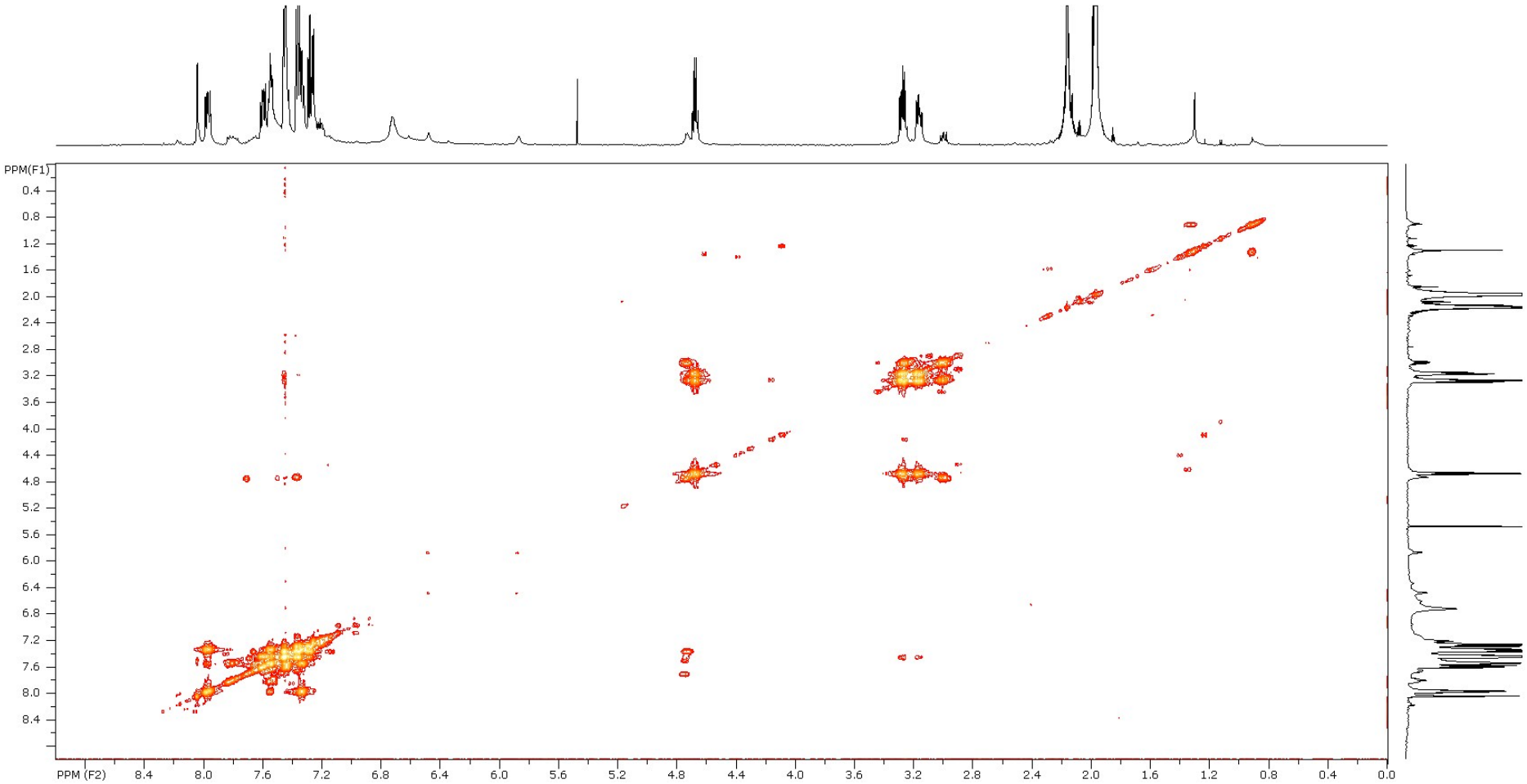

Figure S 25. ^{1}H COSY spectrum of **2a** in acetonitrile-d_3.

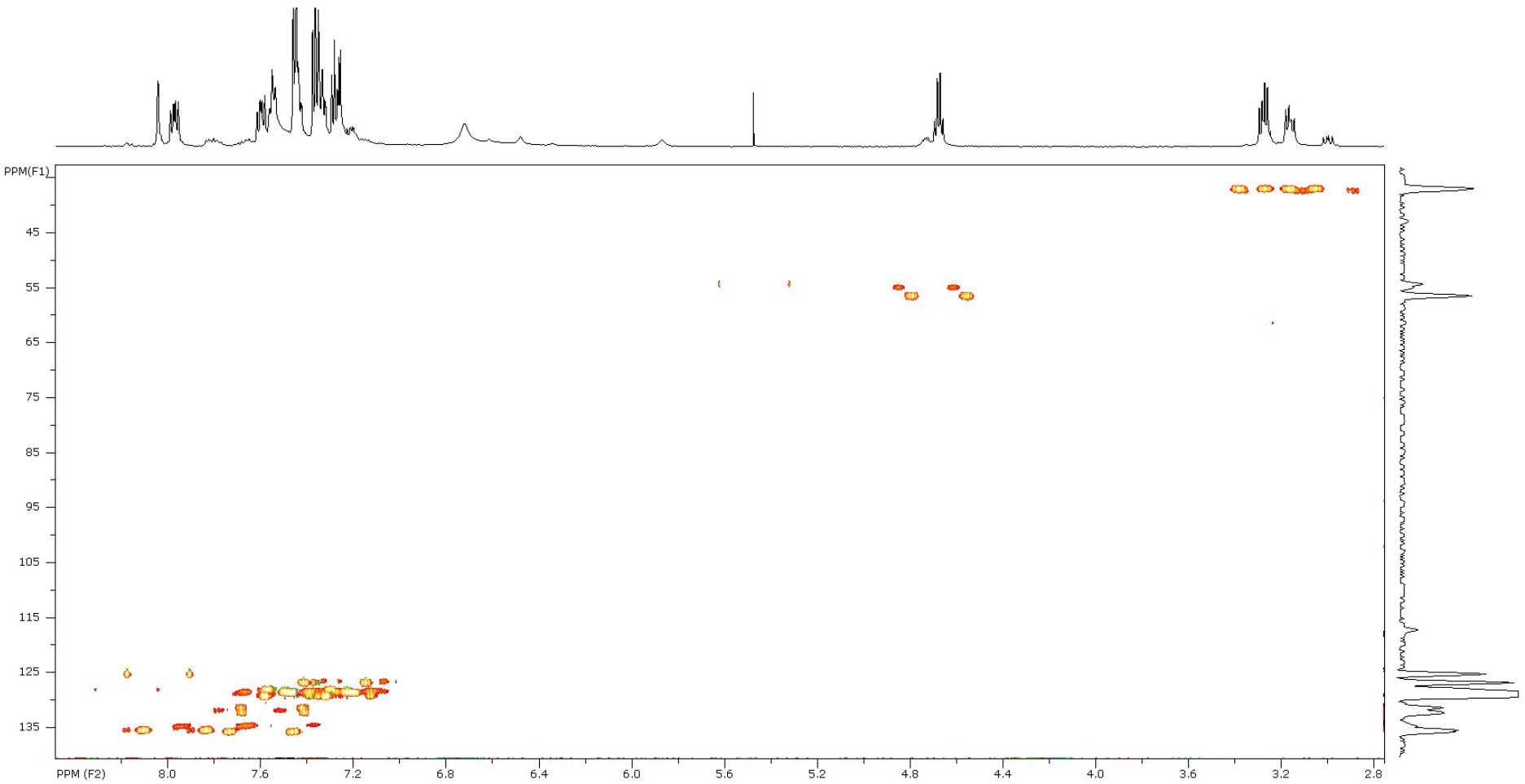

Figure S 26. F_2-coupled ^{1}H, ^{13}C HSQC spectrum of **2a** in acetonitrile-d_3.

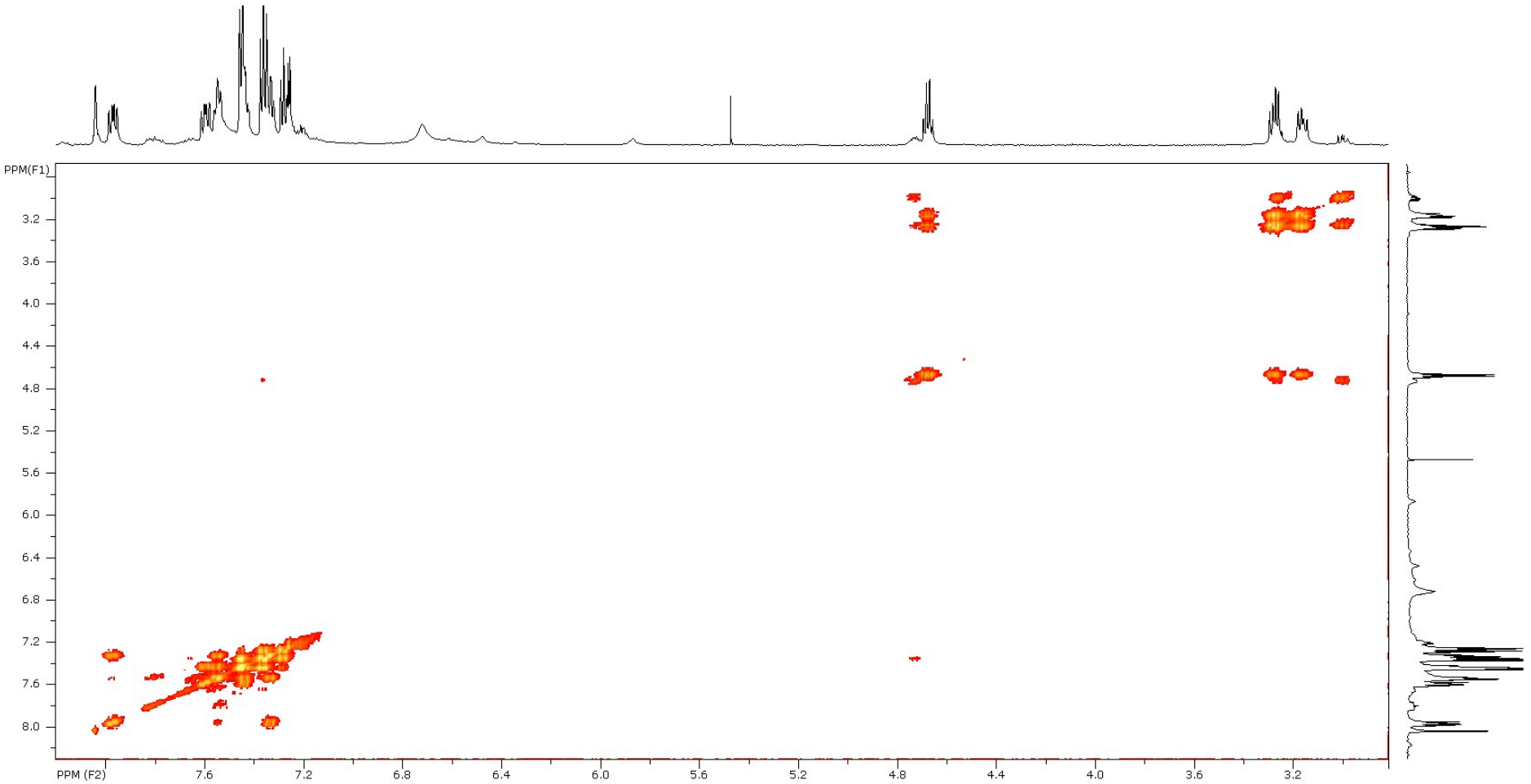

Figure S 27. ^{1}H COSY spectrum of **2a** in acetonitrile-d_3

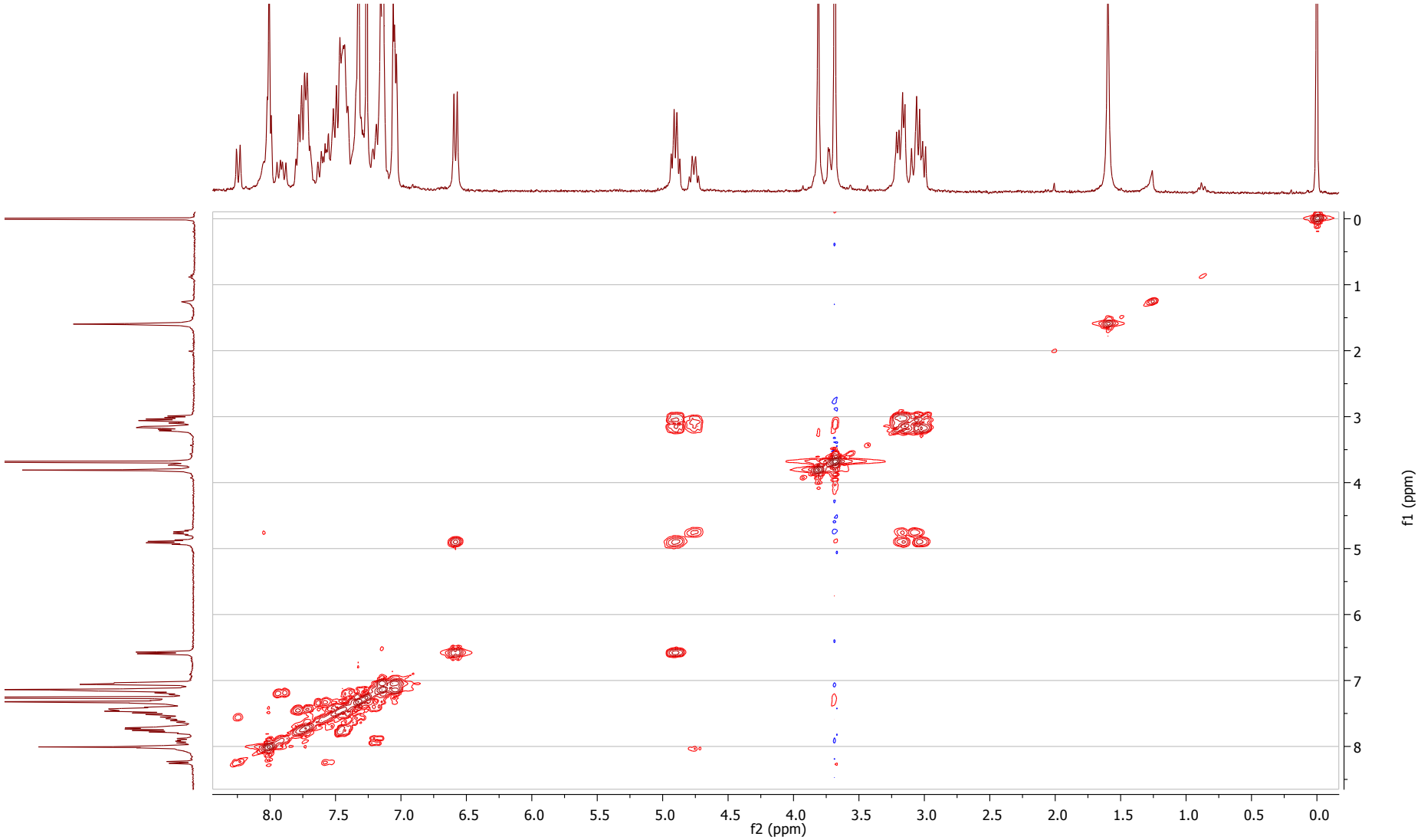

Figure S 28. ^{1}H COSY spectrum of **2b** in chloroform-d_1.

Table S 2. Diffusion coefficients (*D*) from DOSY measurements

Compound	*D* / $m^2 s^{-1}$	
	chloroform	30% acetonitrile/chloroform mix
trans-**2a** (dimer)	4.93E–10	5.73E–10
trans-**2b** (monomer)	6.06E–10	/
cis-**2a** (monomer)	/	6.90E-10
Aggregation number[(a)]	1.7 (1.9)	1.6 (1.8)

[(a)] Calculated as ratio of sphere volumes of *trans*-**2a** and *trans*-**2b** or *cis*-**2a**. The sphere volume, *V*, was obtained using the radius (r_H, Chen-corrected[9] for solvent size) calculated from the following equation: $r_H = kT/(c\pi\eta D)$, where $c = 6/(1+0.695\times(r_{solv}/r_H)\text{^}2.234)$. The values in parenthesis are not corrected for solvent size ($c = 6$). The chloroform molecule radius, r_{solv}, was approximated as 3.5 Å. The viscositiy of chloroform[8] was taken as 0.539 mPa s, and for acetonitrile 0.344 mPa s (http://www.ddbst.com/). The viscosity of the solvent mixture, 0.451 mPa s, was calculated by the following equation for ideal solvent mixtures: $\ln\eta_{mix} = x_A\ln\eta_A + x_B\ln\eta_B$.

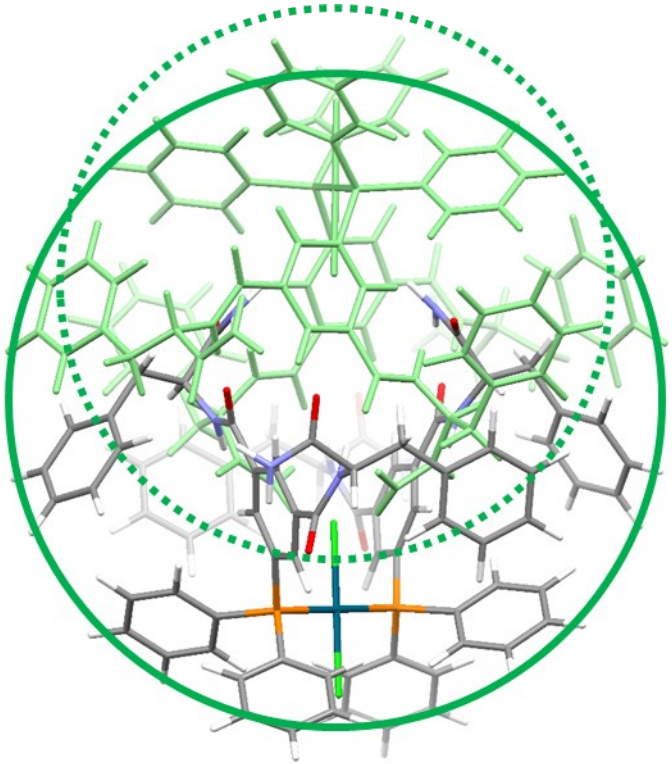

Figure S 29. Calculated sphere size of the monomer (*d* = 15 Å, dashed circle) and dimer (*d* = 18 Å, full circle) in chloroform, superimposed on a DFT optimised dimeric structure of **2a**. One complex molecule is coloured green for clarity.

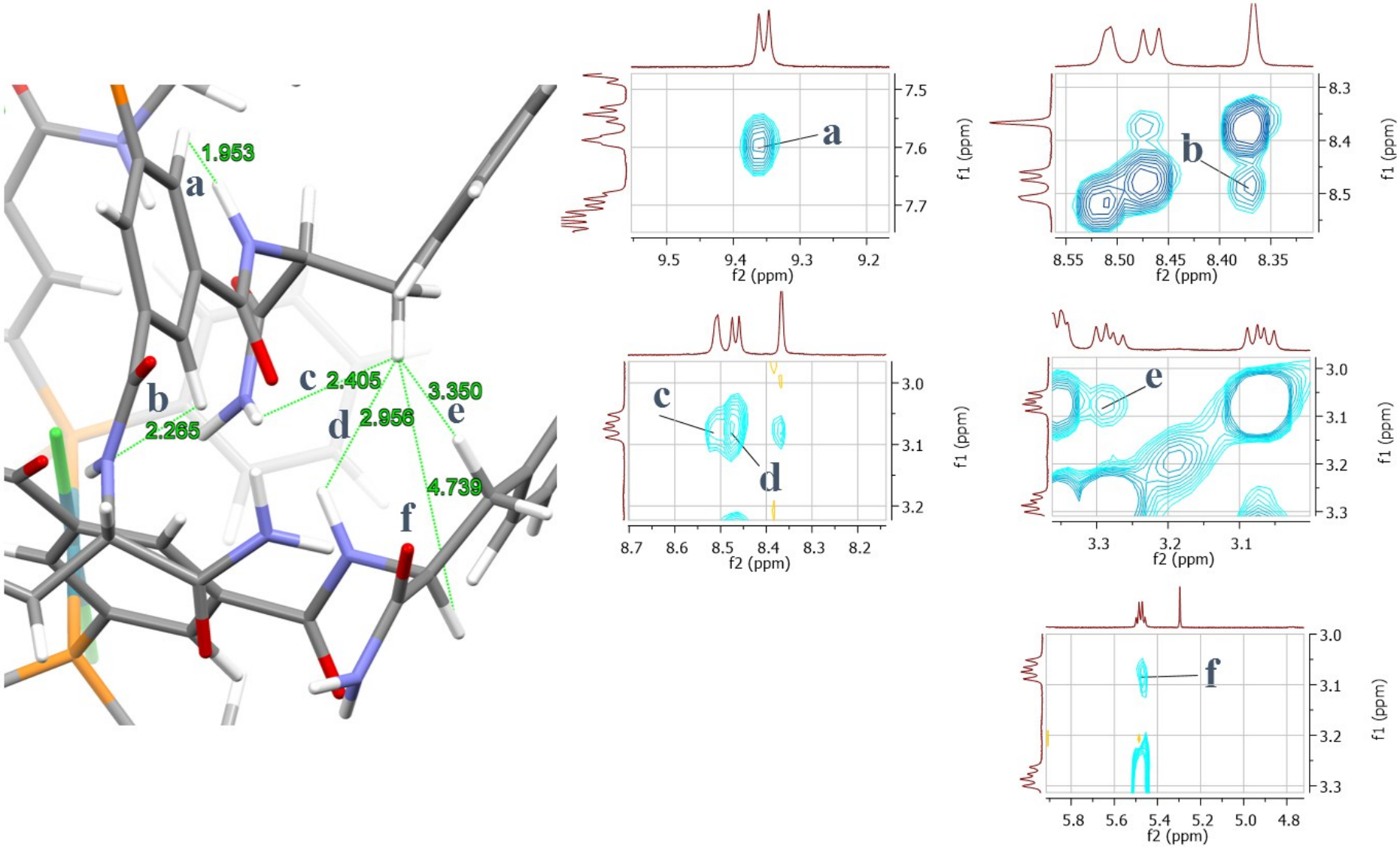

Figure S 30. Intercepts of chosen NOESY (chloroform) contacts in comparison to the DFT optimised dimer of **2a** (distances in Å), in support to the proposed calculated structure.

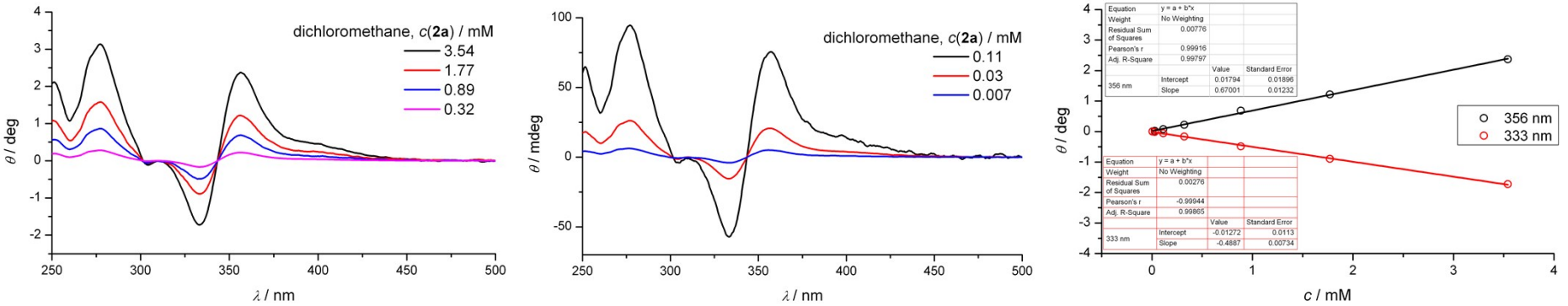

Figure S 31. Variable concentration CD of **2a** in dichloromethane, showing linear relationship in a wide concentration range (0.007–3.54 mM). The data are corrected for 1 cm path length.

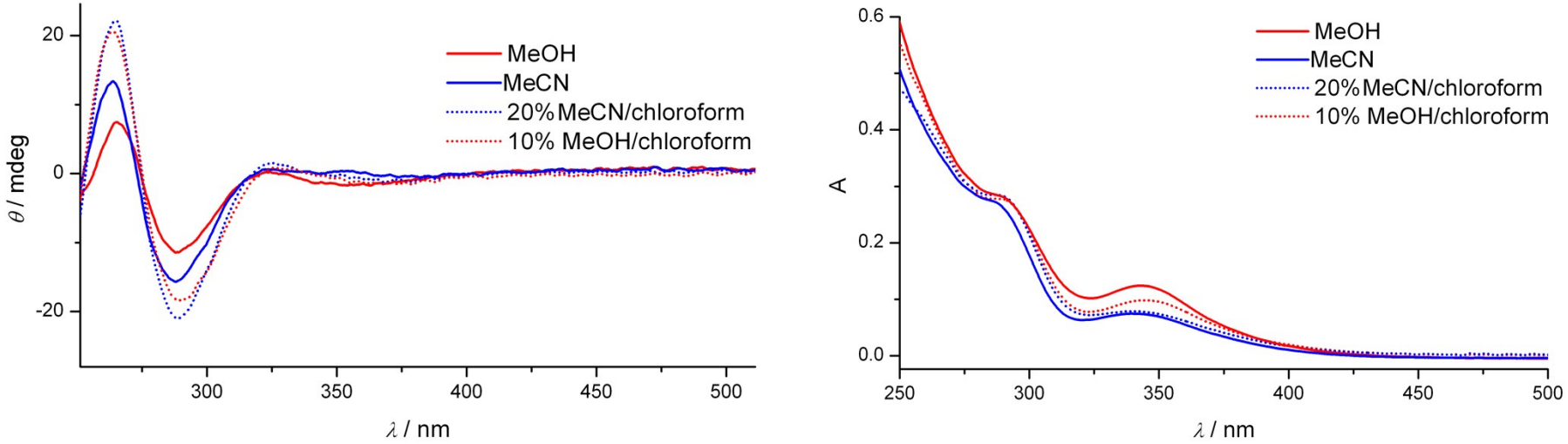

Figure S 32. CD and UV spectra of **2a** in different solvents and solvent mixtures (15 μM). Comparison of the pure and mixed solvent CD spectra indicates cis-configuration of the palladium, since in pure solvents, the complex is mostly *cis*-configured (^{31}P NMR, UV).

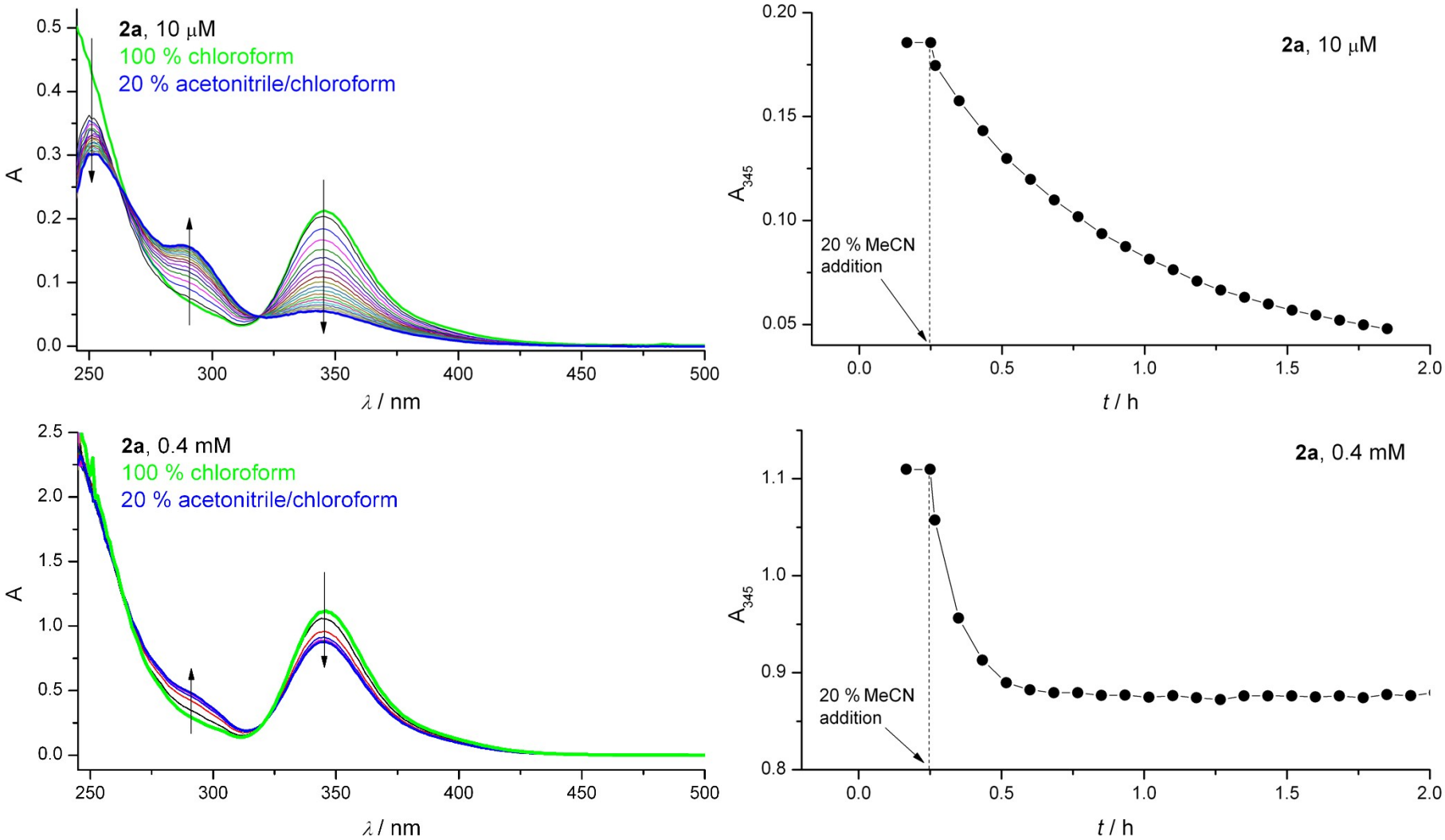

Figure S 33. Time-course UV-Vis measurements of **2a** in chloroform, upon 20 % acetonitrile addition. The chloroform (green line, top left) and the final spectra (blue line, top left) are indicative of the trans- and cis-isomers, respectively. The spectra at higher concentration (bottom left) indicate incomplete isomerisation (e.g. a cis-trans equilibrium is obtained under the given experimental conditions). The chloroform spectra are corrected for concentration.

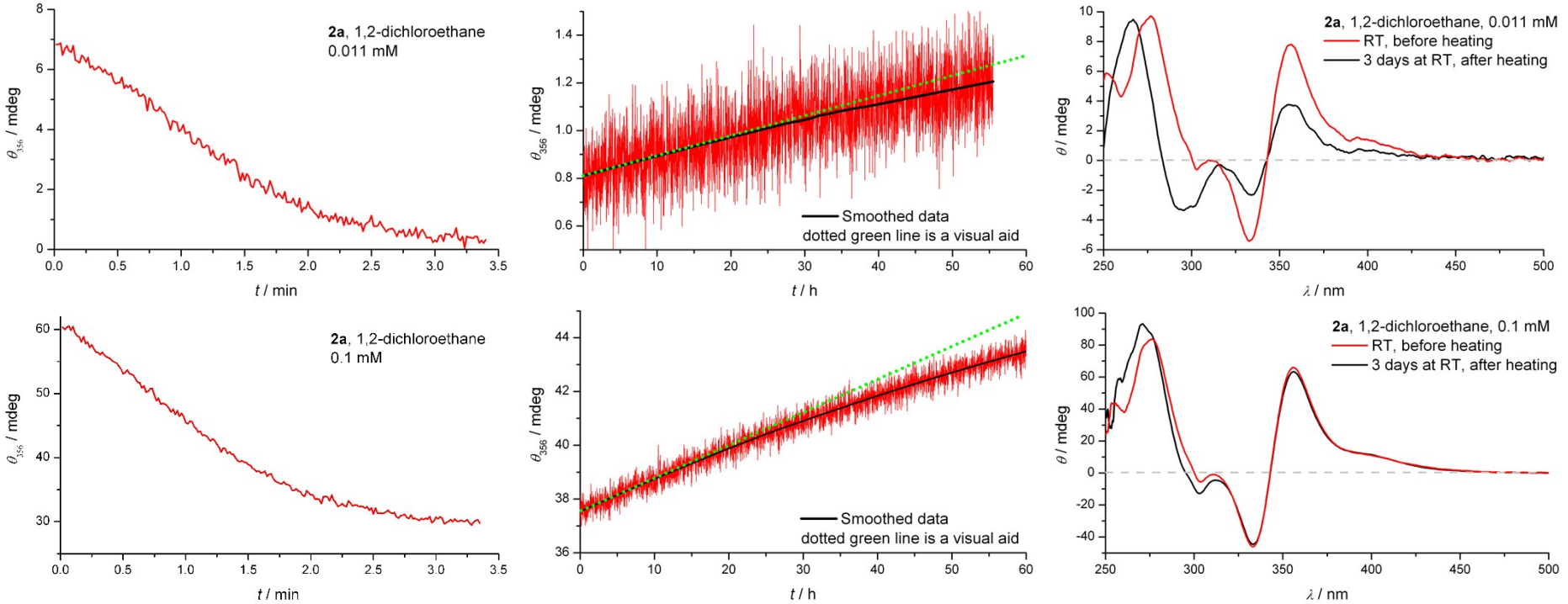

Figure S 34. Time-dependant reduction of the couplet intensity (left) of **2a**, in 1,2-dichloroethane at two concentrations, upon heating for 3.5 min at 70 °C. The measurement was started immediately after putting a cuvette in a preheated Peltier thermostat. After 3 min, the couplet almost completely vanished at lower concentration, but was only halved at higher concentration, indicating different equilibrium at 70 °C. Time-dependant increase of the couplet intensity (middle) at 25 °C, after heating for 3.5 min at 70 °C (subsequently cooled in a water flow for 2 min, and then thermostated at 25 °C), shows dimer reassembly process. CD spectra before and after heating and standing at RT for 3 days (right). Almost complete reassembly is visible at higher concentration. At lower concentration, approximately 1/2 of the complex is in a dimeric form (concluded from the linear relationship of the couplet intensity with concentration).

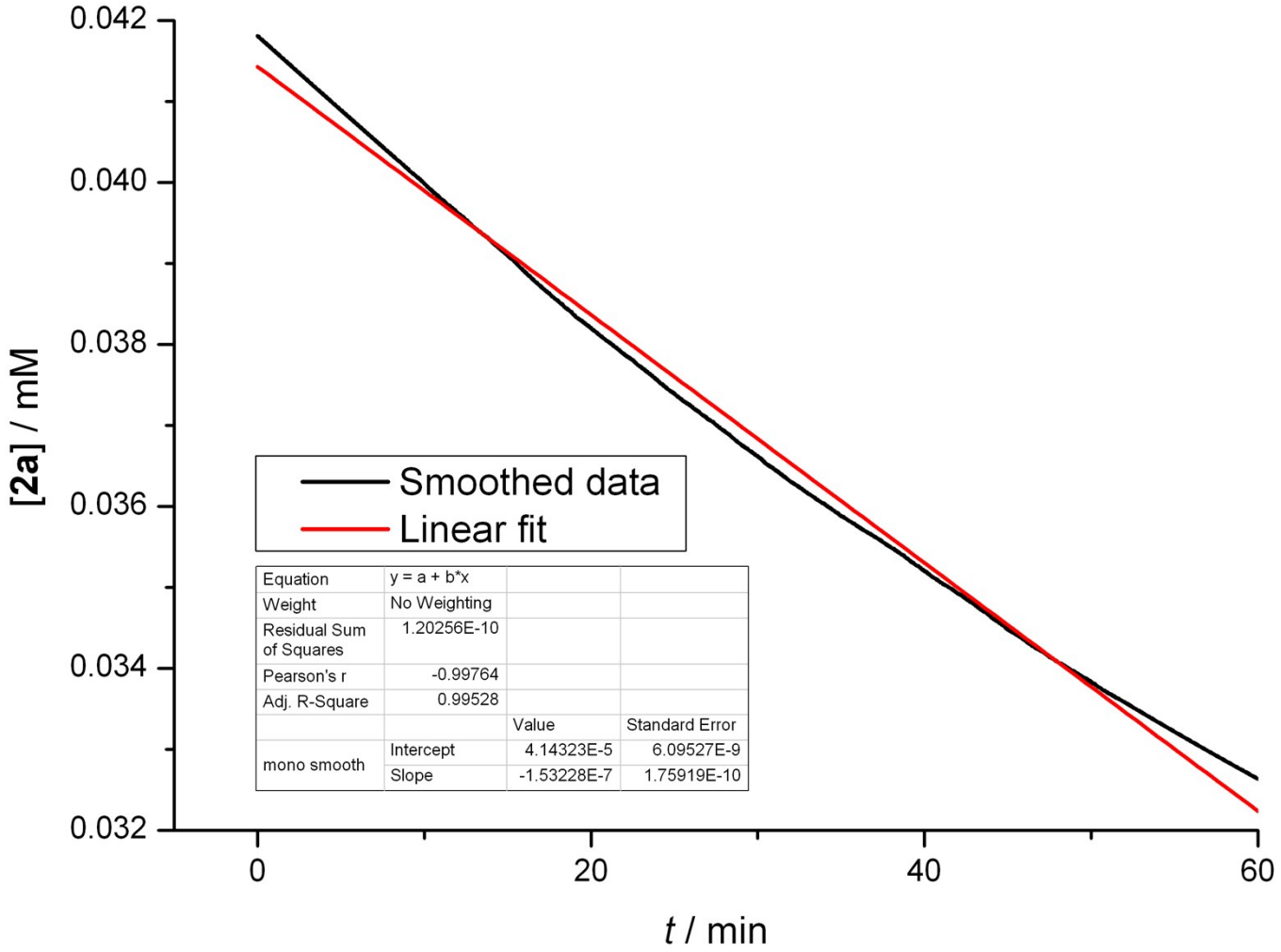

Equation	y = a + b*x		
Weight	No Weighting		
Residual Sum of Squares	1.20256E-10		
Pearson's r	-0.99764		
Adj. R-Square	0.99528		
		Value	Standard Error
mono smooth	Intercept	4.14323E-5	6.09527E-9
	Slope	-1.53228E-7	1.75919E-10

Figure S 35. Time vs. concentration of **2a**, for the dimer reassembly process, after heating to 70°C and quick cooling to 25 °C, in 1,2-dichloroethane. The concentration data was calculated from the smoothed couplet intensity data (see Figure S 34, middle bottom chart).

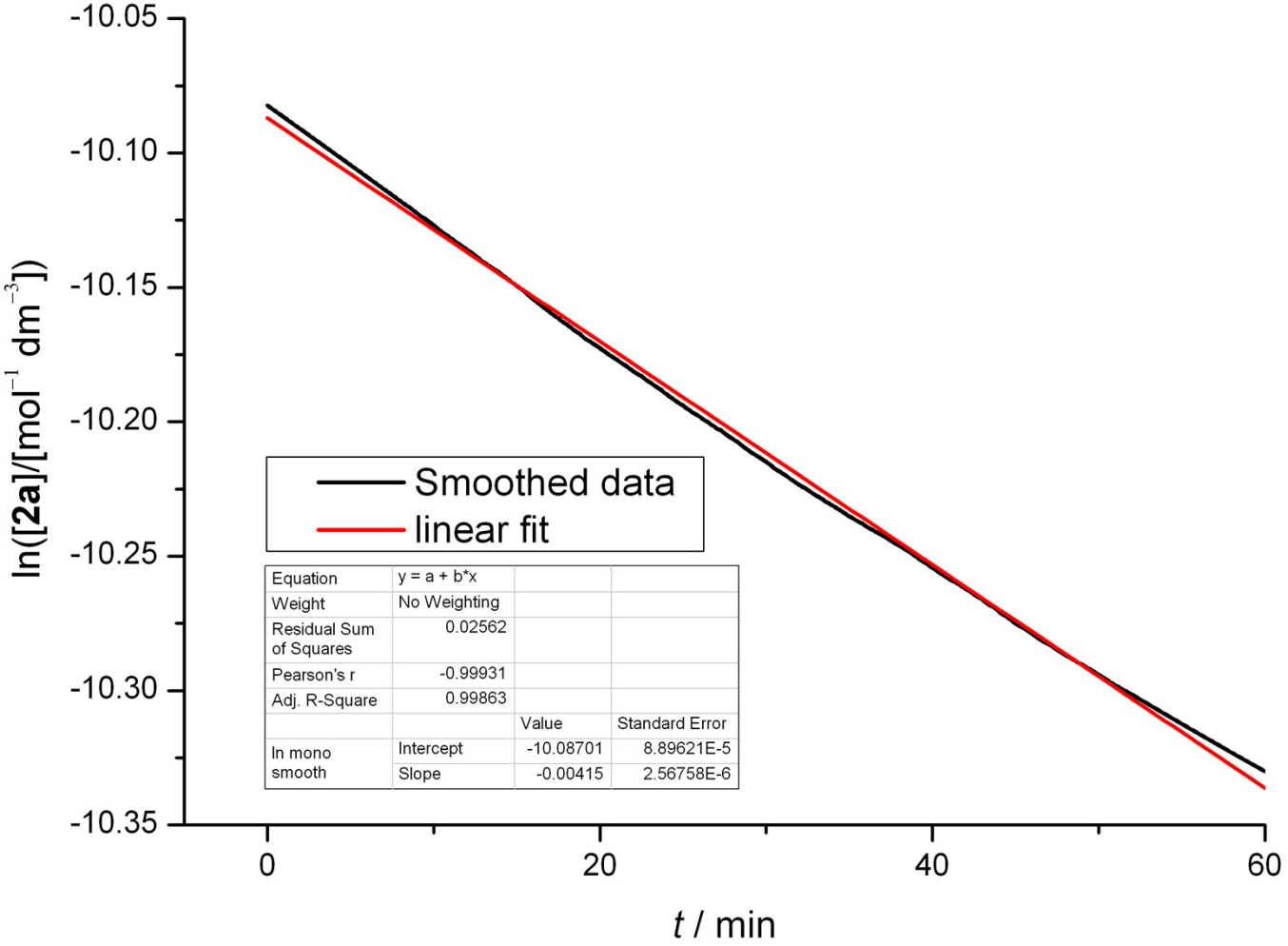

Figure S 36. Time vs. logarithm of **2a** concentration, for the dimer reassembly process, after heating to 70°C and quick cooling to 25 °C, in 1,2-dichloroethane. The concentration data was calculated from the smoothed couplet intensity data (see Figure S 34, middle bottom chart).

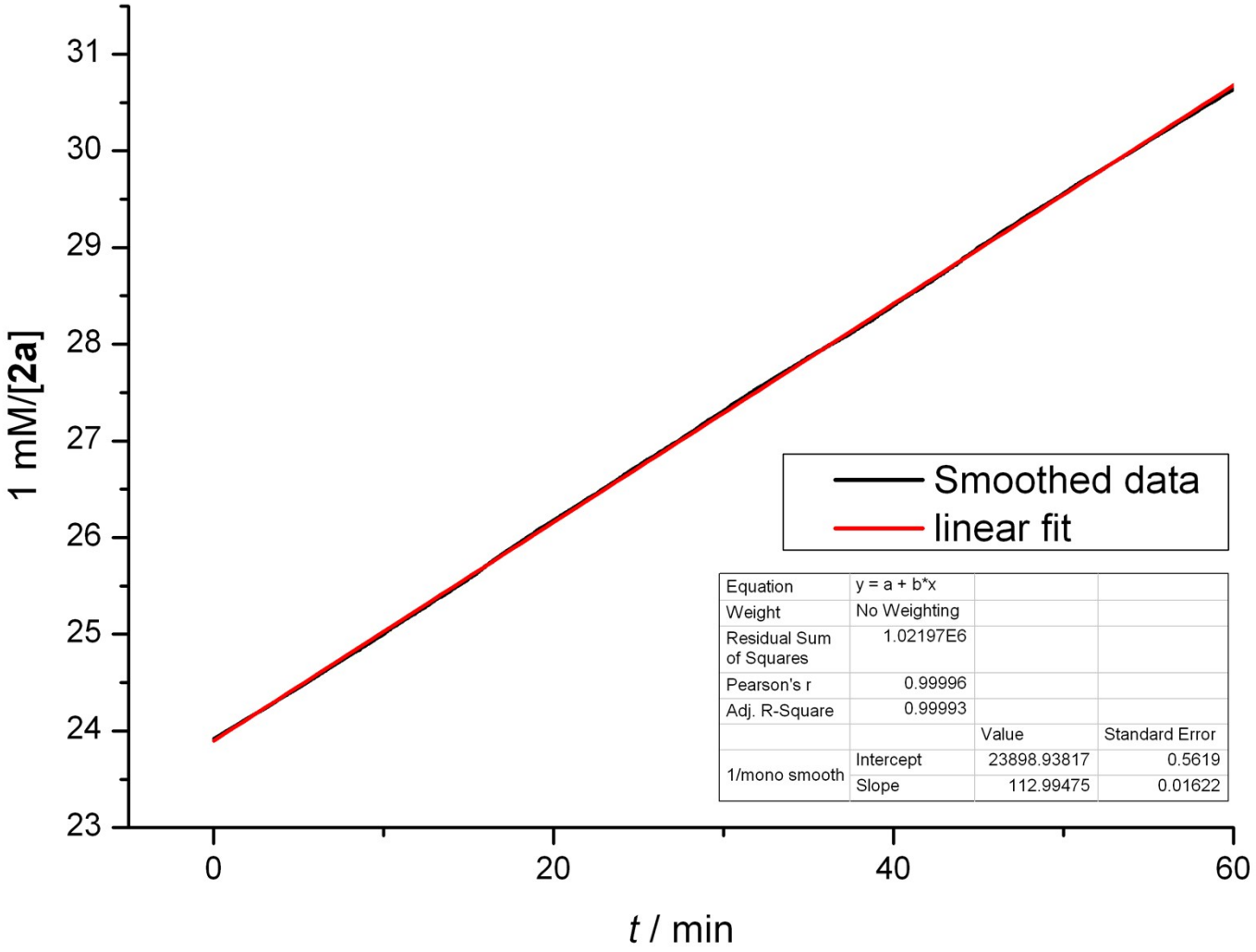

Figure S 37. Time vs. inverse concentration of **2a**, for the dimer reassembly process, after heating to 70°C and quick cooling to 25 °C, in 1,2-dichloroethane, showing the reassembly process is second order in **2a** monomer concentration. The concentration data was calculated from the smoothed couplet intensity data (see Figure S 34, middle bottom chart).

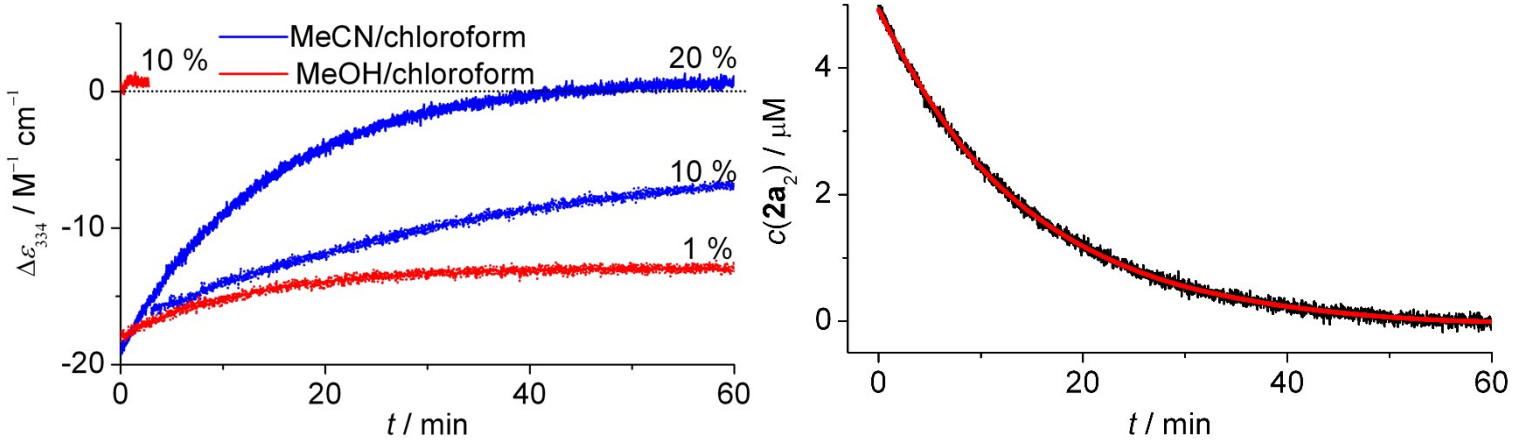

Figure S 38. (left) Reduction of the exciton couplet intensity of **2a** in chloroform (334 nm), upon solvent mixing; (right) time vs. dimer concentration after 20 % acetonitrile addition (calculated from the linear relationship with the couplet intensity (see Figure S 31)). The red line represents smoothed data.

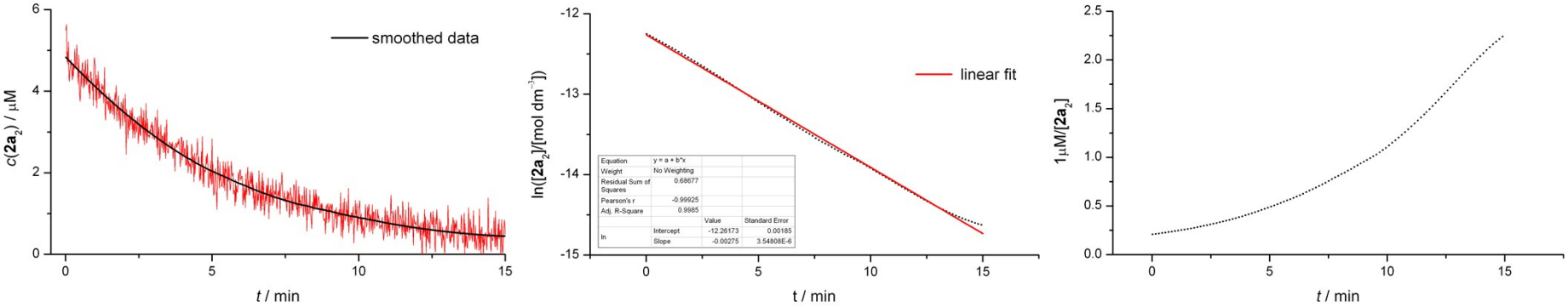

Figure S 39. Time vs. concentration, logarithm, or inverse thereof, respectively, of temperature-induced disassembly of **2a** dimer in 1,1,2,2-tetrachloroethane, recorded immediately after putting cuvette in a preheated Peltiere thermostat at 60°C. Concentration data were calculated from the reduction of the couplet intensity at 358 nm, assuming linear concentration dependence. The best linearity of the data plots (middle) indicates first order reaction for temperature-induced dimer disassembly.

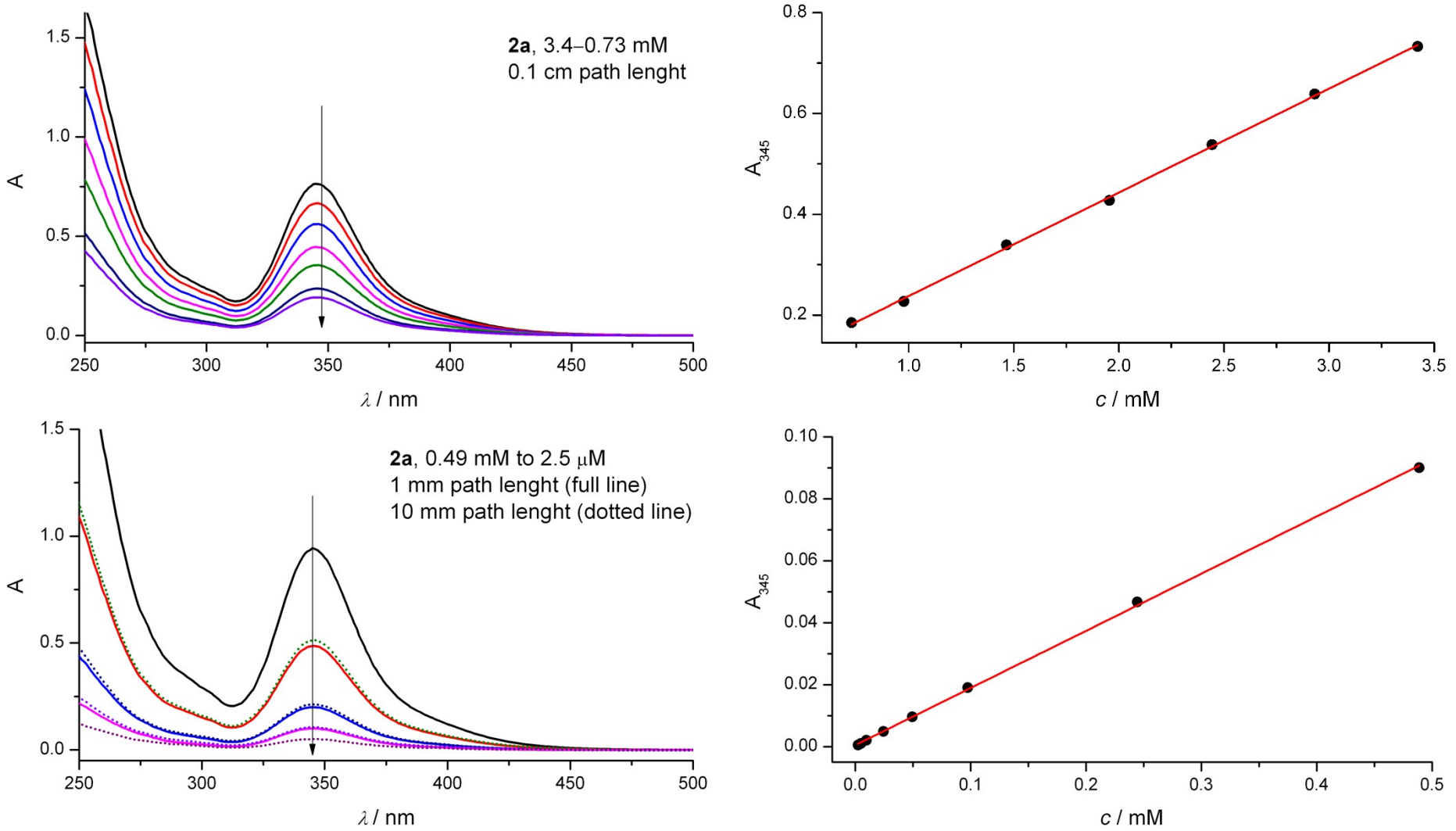

Figure S 40. Variable concentration UV-Vis measurements of **2a** in chloroform, showing linearity throughout a wide concentration range (3.4 mM to 2.5 μM, ε_{345} = 1.9 mM^{-1} cm^{-1}). The concentration vs. absorbance plots are corrected for 0.1 mm path length.

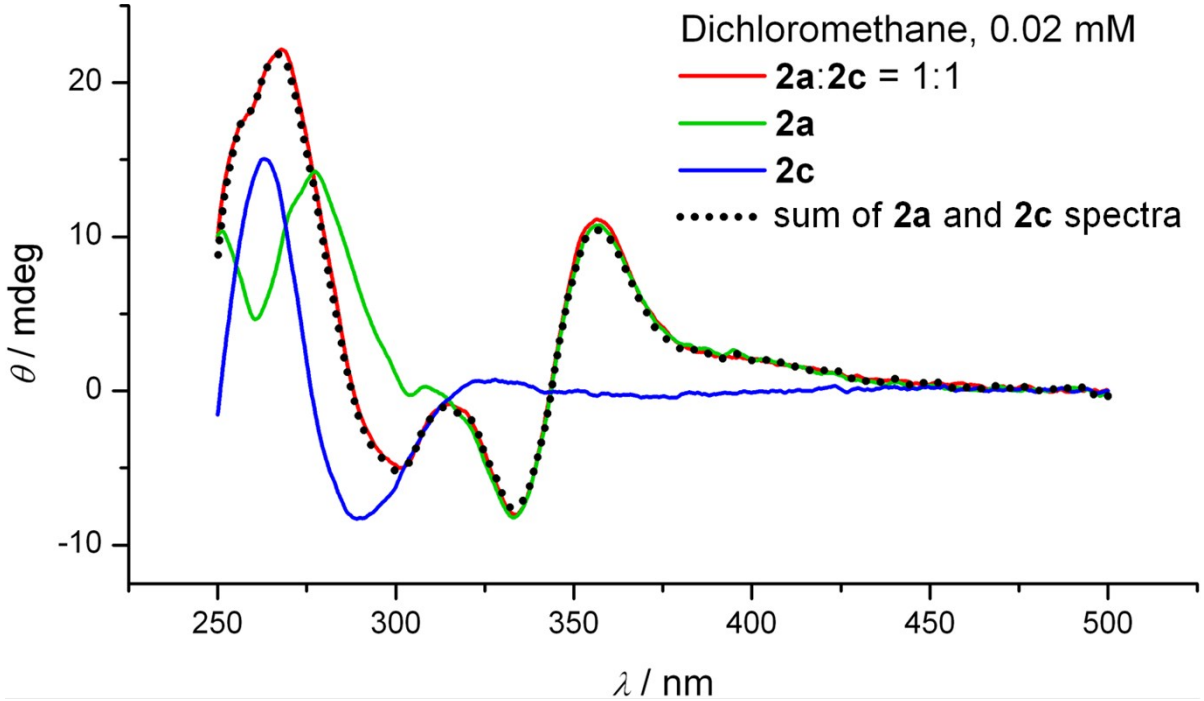

Figure S 41. CD spectra of **2a**, **2c**, and mixture thereof (1 cm quivet). The mixed spectrum is the superposition of pure **2a** and **2c** solutions indicating that the species act independently in solution.

DFT Calculations

As mentioned in the main text, the crystal structure of phenylalanine dimer has not been determined. Therefore, in preparing of initial structures for DFT calculations we relied on educated guess approach and exploited the data from 2D NMR spectrum. Namely, in building of initial structures, we tend to maximize the number of intermolecular H-bonds and π-π stacking interactions which are the driving forces for dimerization process. Several initial structures that were generated by this approach are optimized in gas phase using semiempirical PM6[10] model. Selected lowest energy structures are optimized in the chloroform and acetonitrile solution utilizing SMD/M062X/6-31G(d,p),Def2-TZVP theoretical model.[11,12] Symmetry constraints are not imposed during optimization, however, tight geometry convergence criteria, and more accurate numerical integration grid (grid=ultrafine) are used. Although geometry optimization was performed without symmetry constraints, all dimeric structures of **2a** resembles near D2 symmetry. Vibrational analysis has been done for all structures to confirm that they are minima on the potential energy surface. Calculation of dimerization free energy and free energy difference between diastereomers is carried out at the SMD/M062X/6-311++G(3df,2p),Def2-TZVP//SMD/M062X/6-31G(d,p),Def2-TZVP level. Calculation of UV-VIS and CD spectra is performed utilizing time-dependent density functional theory (TDDFT) with the SMD/CAM-B3LYP[13] exchange correlation functional along with 6-31G(d,p),Def2-TZVP basis sets on solution phase geometry of chloroform solution. All calculations have been performed with the Gaussian 09 program package.[14] The structure of **2a** dimer in chloroform solution is presented in man text of the manuscript (Figure 7) whereas diastereomer of **2a** is presented on Figure S 42a,b. Calculated and experimental UV/VIS spectra are presented on Figure 8 of the main text. The maximum absorbance on calculated CD spectra corresponds to a wavelength of 322 nm. This is somewhat lower than the maximum absorption wavelength in experimental spectra (≈344 nm) but still in a good agreement with it. The absorption UV/VIS spectra of **2a** monomer exhibits maximal absorption at 321.5 nm, which correspond to HOMO-2 -> LUMO transition (orbitals are presented on Figure S 43). When two monomers of **2a** are brought into close spatial proximity to form a **2a** dimer, the CD spectra exhibits typical characteristic of an exciton coupled systems or Davydov splitting (Figure 8 and Figure S 42c). The experimental and calculated spectra are in a good agreement, particularly related to the assignment of absolute configuration (P-helical chirality).

In Scheme 2 of the main text we proposed different *cis*-*trans* equilibria that could lead to a formation of dimer **2a.** To find out what could be the driving force for dimer formation in chloroform and absence of corresponding dimerization in acetonitrile, we compared the stability of *cis* and *trans* isomers of monomer **2a** in both, acetonitrile and chloroform solution. Further we calculated the dimerization free energy in both solvents. Results are presented in Table S 3.

It appears that *cis* isomer is more stable in both solvents. However, *cis* isomer exhibits substantially greater stability in acetonitrile than in chloroform solution. Calculated dimerization free energy in chloroform of –52.7 kJ mol^{-1} imply that process is exergonic, whereas in acetonitrile solution the dimerization free energy is positive (25.5 kJ mol^{-1}) indicating that formation of dimer is energetically unfavourable, which is in agreement with experimental findings.

Table S 3. Relative stability of *cis* and *trans* monomers of **2a** together with dimerization free energy in chloroform and acetonitrile solution.

	Relative stability (Δ*G*) / kJ mol^{-1}		Dimerisation energy[a] (Δ*G*) / kJ mol^{-1}	
	Chloroform	Acetonitrile	Chloroform	Acetonitrile
cis-**2a** (monomer)	0.0	0.0		
trans-**2a** (monomer)	20.1	47.7		
trans-**2a** (dimer)			–52.7	25.5

[a] Dimerisation free energy is calculated as a free energy difference between dimer and two *cis* monomers at infinite distance.

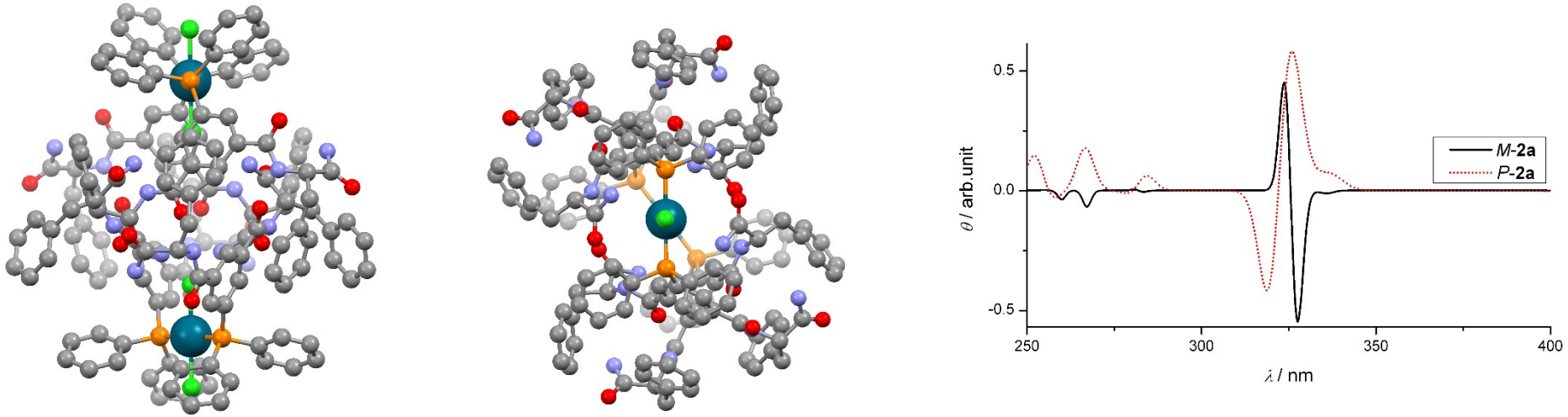

(a) (b) (c)

Figure S 42. (a) Side and (b) top view of DFT optimised (chloroform) *M*-atropoisomer of **2a** dimer (diastereomeric in nature due to L-configuration of the phenylalanine). (c) The calculated circular dichroism of two **2a** dimeric atropoisomers (*P* or *M*), showing opposite CD signals. The experimental measurements suggest *P*-isomer is predominant in solution (positive exciton couplet around 350 nm, Figure S 31), also confirmed by the energy calculations, with the *M*-isomer being less stabile for 12.5 kJ/mol (0.7 % present in solution calculated using Boltzman distribution).

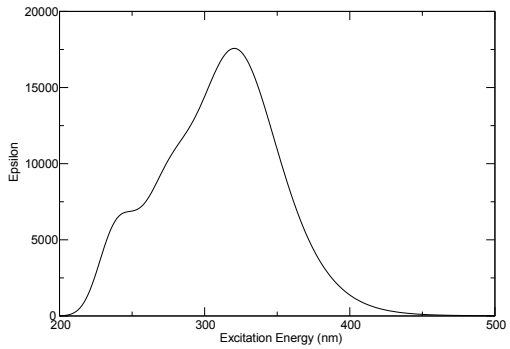

UV/VIS

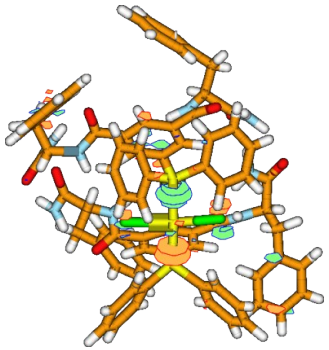

HOMO-2

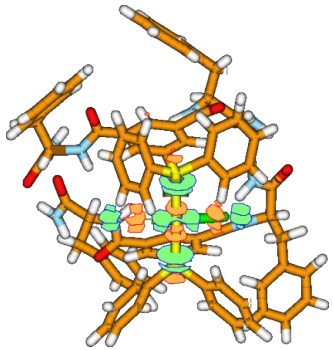

LUMO

Figure S 43. Calculated UV/VIS spectra of **2a** monomer and orbitals associated with transition at 321.5 nm.

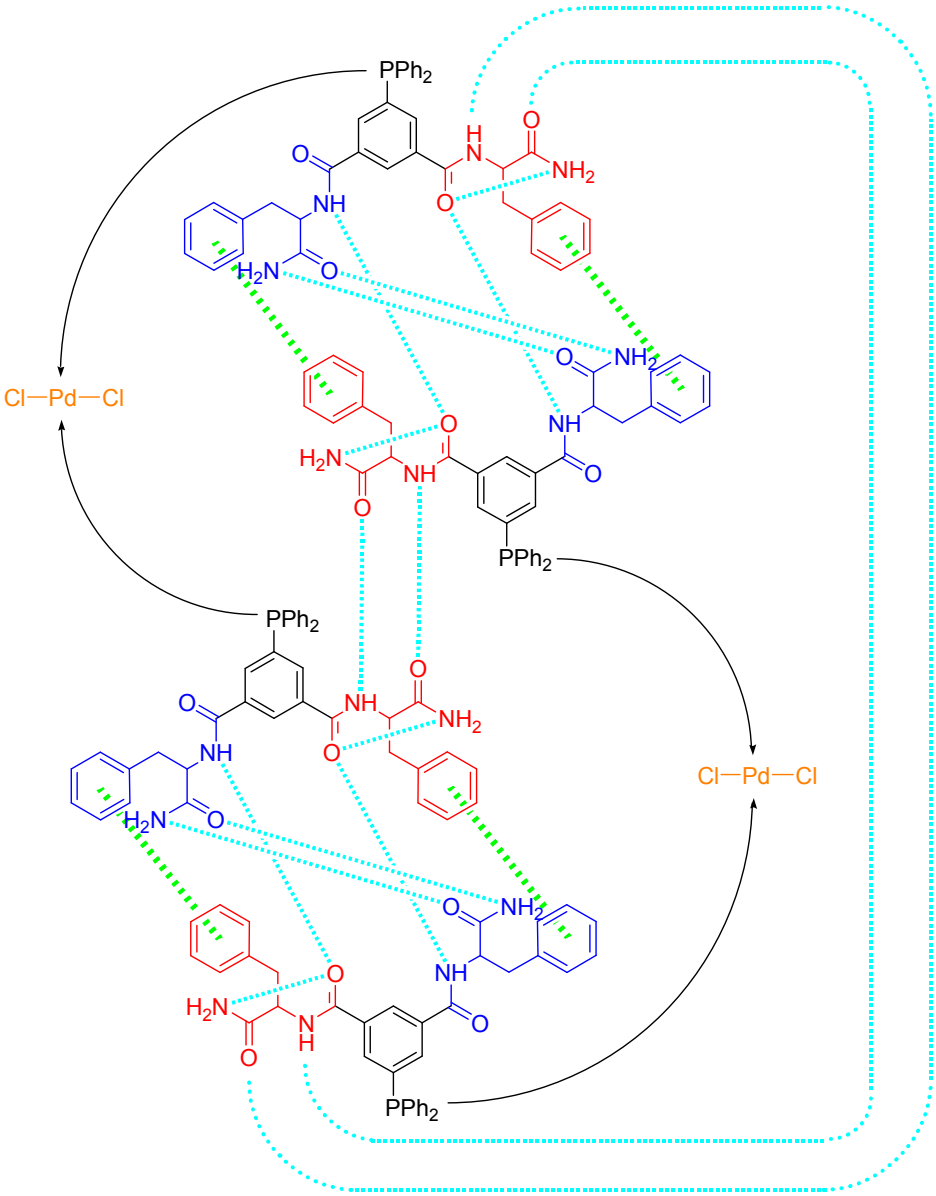

Figure S 44. Hydrogen bonding (dashed light blue) and aromatic stacking (dashed green) scheme in the DFT optimised **2a** dimer supports the 16 hydrogen bonds and aromatic stacking concluded from the NMR spectra.

X-ray Measurements

We were able to obtain single crystals of **2a** in two separate experiments: 1) diethyl-ether vapour diffusion into dichloromethane solution of **2a** at 4 °C; 2) slow evaporation of deuterochloroform solution of **2a** at room temperature. In both cases, two polymorphs were obtained – hexagonal plates and thin needles. The size and the appearance of the crystals were satisfactory, however unfortunately, we were not able to collect the single crystal data due to the extremely poor diffraction thereof.
Single crystals of *cis*-**2c** were obtained from acetonitrile solution.

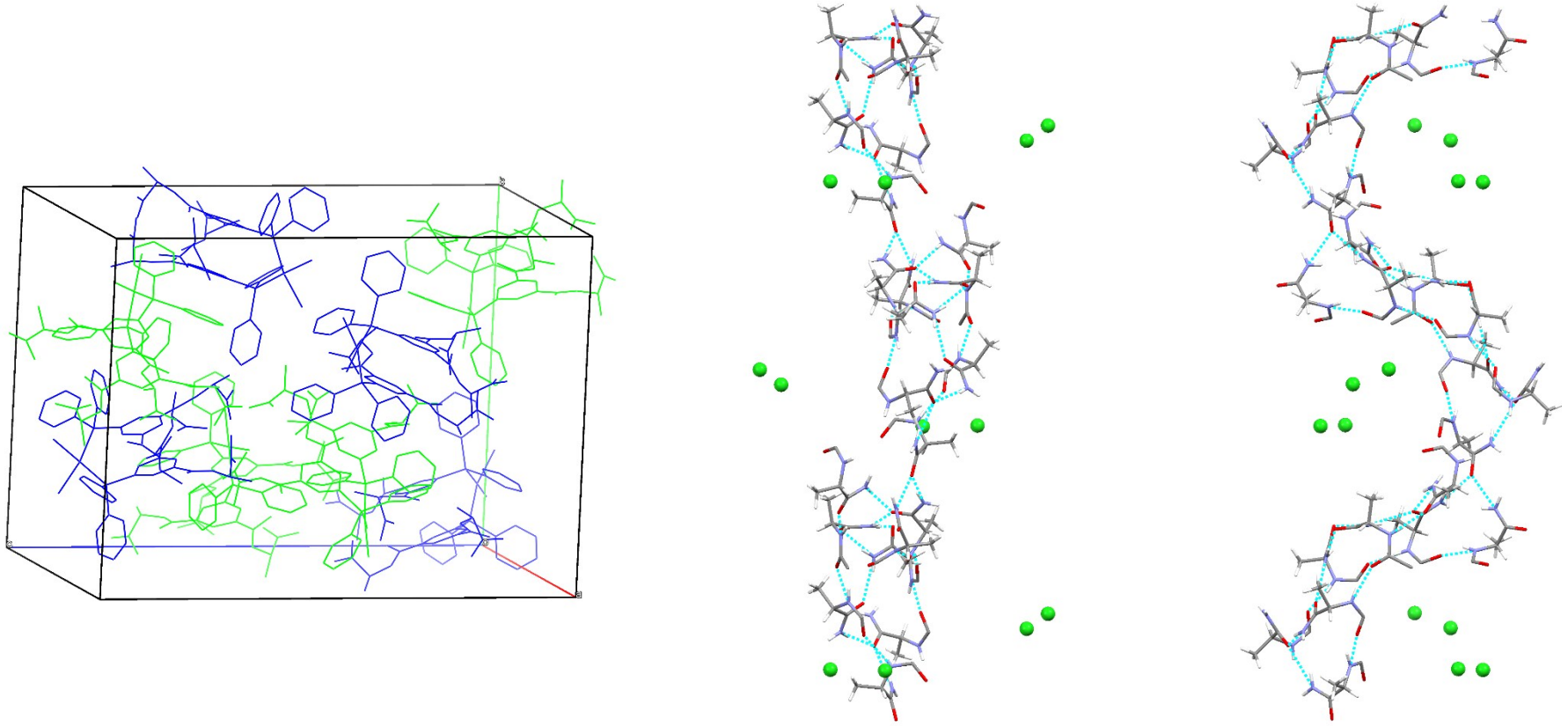

(a) (b) (c)

Figure S 45. (a) Crystal packing of **2c** (molecules coloured by symmetry equivalence). (b,c) orthogonal side views of amino acids forming a flattened *P*-helical hydrogen bonding pattern, expanding to a 3D array through hydrogen bonding with chloride atoms. Palladium triphenylphosphine moieties are omitted for clarity.

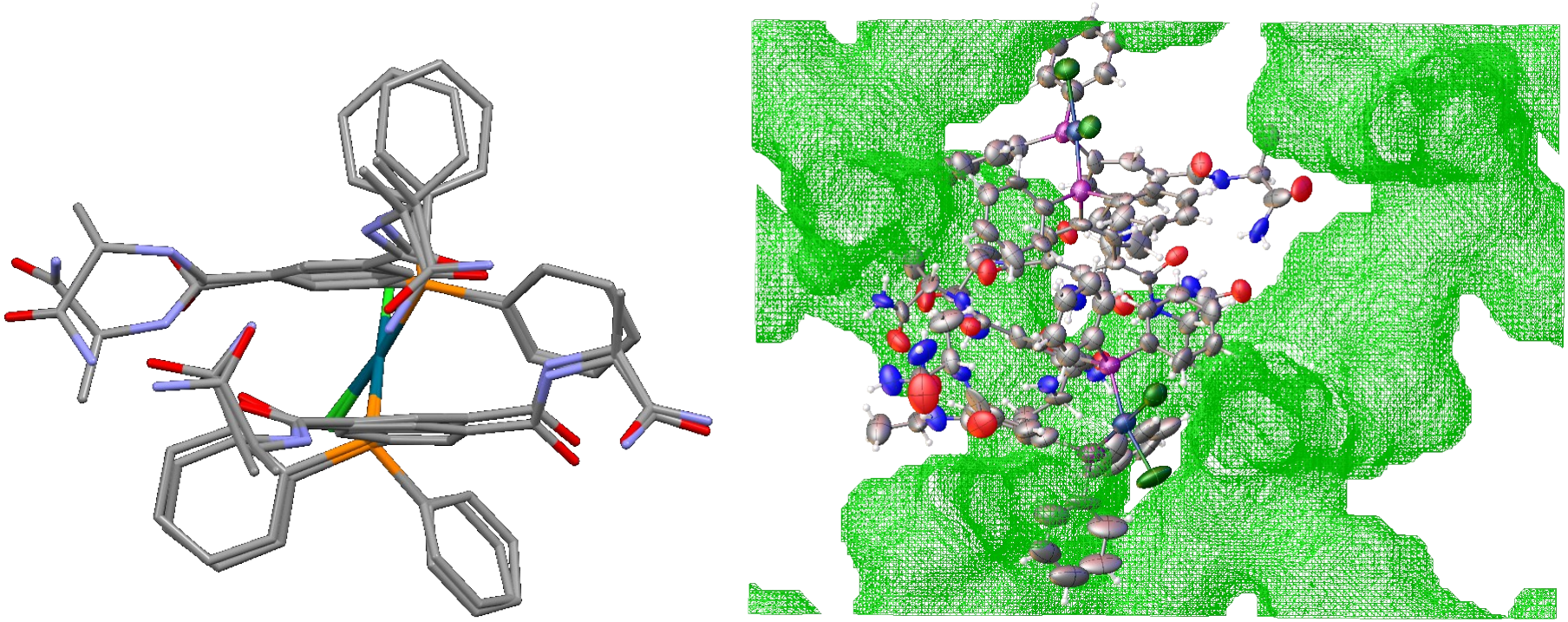

(a) (b)

Figure S 46. (a) Overlapped molecular structures of the two conformers in the crystal structure of **2c**; (b) A significant part of the unit cell (green mesh) is occupied by disordered solvent, contributing to the limited resolution to which the crystals diffracted.

Table S 4. Crystal data and structure refinement for *cis*-**2c**.

Empirical formula	$C_{52}H_{54}Cl_2N_8O_8P_2Pd$
Formula weight	1158.27
Temperature/K	99.98(19)
Crystal system	orthorhombic
Space group	$P2_12_12_1$
a/Å	18.7533(11)
b/Å	21.7745(11)
c/Å	29.714(2)
α/°	90
β/°	90
γ/°	90
Volume/Å^3	12133.6(12)
Z	8
ρ_{calc}g/cm^3	1.268
μ/mm^{-1}	4.217
F(000)	4768.0
Crystal size/mm^3	0.19 × 0.071 × 0.067
Radiation	CuKα (λ = 1.54184)
2*Θ* range for data collection/°	6.896 to 105.32
Index ranges	-19 ≤ h ≤ 17, -22 ≤ k ≤ 18, -30 ≤ l ≤ 29
Reflections collected	17899
Independent reflections	11917 [R_{int} = 0.1918, R_{sigma} = 0.1449]
Data/restraints/parameters	11917/324/1168
Goodness-of-fit on F^2	1.012
Final R indexes [I>=2σ (I)]	R_1 = 0.0898, wR_2 = 0.2223
Final R indexes [all data]	R_1 = 0.1264, wR_2 = 0.2518
Largest diff. peak/hole / e Å^{-3}	1.17/-0.56
Flack parameter	0.059(18)

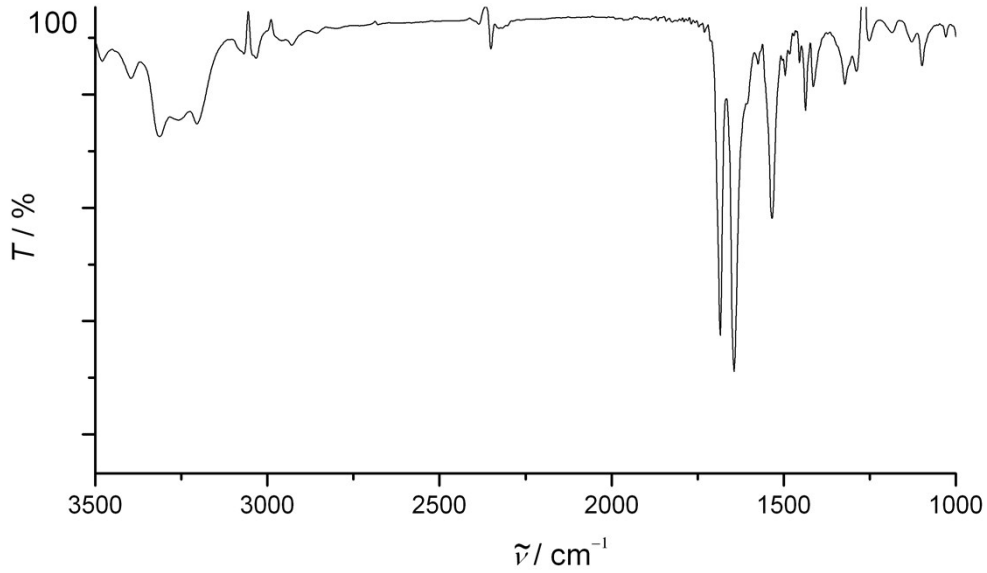

Figure S 47. IR (dichloromethane, 11 mM) spectrum of **2a**.

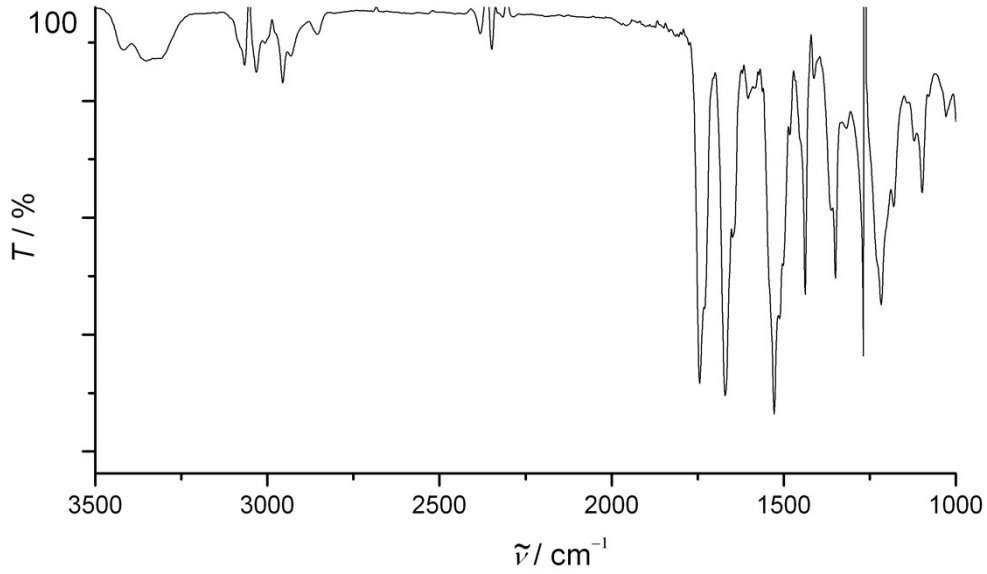

Figure S 48. IR (dichloromethane, 10 mM) spectrum of **2b**.

References

1 O. V. Dolomanov, L. J. Bourhis, R. J Gildea, J. A. K. Howard, and H. Puschmann, *J. Appl. Cryst.* **2009**, 42, 339–341.
2 G. M. Sheldrick, *Acta Cryst*. **2008**, A64, 112–122.
3 G. M. Sheldrick, *Acta Cryst.* **2015**, C71, 3–8.
4 B. Rees, L. Jenner, and M. Yusupov, *Acta Cryst.* **2005**, D61, 1299–1301.
5 Z. Kokan and S. I. Kirin, *Eur. J. Org. Chem.* **2013**, 8154–8161.
6 E. S. Stevens, N. Sugawara, G. M. Bonora, and C. Toniolo, *J. Am. Chem. Soc.* **1980**, 102, 7048–7050.
7 Z. Kokan, B. Perić, G. Kovačević, A. Brozovic, N. Metzler-Nolte, and S. I. Kirin, *Eur. J. Inorg. Chem.* **2017**, 3928–3937.
8 D. Li, G. Kagan, R. Hopson, and P. G. Williard, *J. Am. Chem. Soc.* **2009**, 131, 5627–5634.
9 H.-C. Chen and S.-H. Chen, *J. Phys. Chem.* **1984**, 88, 5118–5121.
10 J. J. P. Stewart*, J. Mol. Model*. **2007**, 13, 1173–213.
11 Y. Zhao, D. G. Truhlar, *Theor. Chem. Acc*. **2006**, 120, 215–241.
12 A. V. Marenich, C. J. Cramer, and D. G. Truhlar, *J. Phys. Chem. B,* **2009**, 113, 6378–6396.
13 T. Yanai, D. Tew, and N. Handy, *Chem. Phys*. Lett., **2004**, 393, 51–57.
14 Gaussian 09, Revision A.02, M. J. Frisch, G. W. Trucks, H. B. Schlegel, G. E. Scuseria, M. A. Robb, J. R. Cheeseman, G. Scalmani, V. Barone, G. A. Petersson, H. Nakatsuji, X. Li, M. Caricato, A. Marenich, J. Bloino, B. G. Janesko, R. Gomperts, B. Mennucci, H. P. Hratchian, J. V. Ortiz, A. F. Izmaylov, J. L. Sonnenberg, D. Williams-Young, F. Ding, F. Lipparini, F. Egidi, J. Goings, B. Peng, A. Petrone, T. Henderson, D. Ranasinghe, V. G. Zakrzewski, J. Gao, N. Rega, G. Zheng, W. Liang, M. Hada, M. Ehara, K. Toyota, R. Fukuda, J. Hasegawa, M. Ishida, T. Nakajima, Y. Honda, O. Kitao, H. Nakai, T. Vreven, K. Throssell, J. A. Montgomery, Jr., J. E. Peralta, F. Ogliaro, M. Bearpark, J. J. Heyd, E. Brothers, K. N. Kudin, V. N. Staroverov, T. Keith, R. Kobayashi, J. Normand, K. Raghavachari, A. Rendell, J. C. Burant, S. S. Iyengar, J. Tomasi, M. Cossi, J. M. Millam, M. Klene, C. Adamo, R. Cammi, J. W. Ochterski, R. L. Martin, K. Morokuma, O. Farkas, J. B. Foresman, and D. J. Fox, Gaussian, Inc., Wallingford CT, 2016.